ADENO-ASSOCIATED VIRUS VECTORED IMMUNOPROPHYLAXIS OF HUMAN MALARIA *PLASMODIUM FALCIPARUM*: MURINE AND NON-HUMAN PRIMATE MODEL

by

Suk Namkung

A thesis submitted to the Johns Hopkins University in conformity with the requirements for the degree of Master of Science

Baltimore, Maryland

April 2019

Abstract

Plasmodium falciparum is a devastating disease. Though different interventions are employed every year, the burden persists, leading to 219 million cases and 435,00 deaths in 2017. The malaria affected regions rely heavily on the anti-malarial drugs such as artemisinin-based combination therapies, and vector control methods. However, recent reports have documented parasites resistant to quinolines and artemisinin-based drugs, and vectors that are resistant to insecticide treatments.

Though decades of research on malaria research has yielded a licensed RTS,S/AS01 malaria vaccine in 2015, the vaccine efficacy only provides a moderate vaccine efficacy (35.9%) in its first year, and wanes completely by year 5. With the increasing reports of resistance in anti-malarial drug and vector control methods, there is a clear evidence for a need of new interventions such as improved vaccines or prophylaxis.

From reports of past and present on immune response against irradiated sporozoites in different animal models and humans, as well as data from the phase 3 clinical trial of RTS,S/AS01, the correlate of protection from sporozoite infection points to neutralizing antibody against the CSP antigen. Extrapolating from the findings, increased amount of CSP neutralizing antibody for an extended period would serve as an ideal vaccine against malaria.

We have investigated expression of high levels of monoclonal antibodies for an extended period by using the vectored immunoprophylaxis (VIP) system through the recombinant Adeno-associated Virus (rAAV) vector and testing malaria protective

efficacy using different animal models. In this thesis we have investigated protective immunity of VIP-AAV induced antibodies that have been recently discovered through Controlled Human Infection Model (CHIM). In transduced mice, MGU-12 monoclonal antibody was expressed at a high concentration and elicited 50% protection.

In preparation for protection challenges, we have characterized VIP-rAAV expression kinetics in a non-human primate *Aotus nancymae* monkeys. When injected with $1x10^{13}$ GC of 2A10-VIP-rAAV, 2/6 monkeys had consistent expression of 2A10 antibodies for >30 weeks while 4/6 Aotus monkeys had only transient antibody titers at around week 3-6. Our results show that improved antibodies can lead to higher rate of protection in VIP-rAAV model but that additional strategies to improve antibody expression consistency may be needed to unleash the full effects of the expressed antibody.

Thesis Advisor: Gary Ketner, PhD

Thesis Reader: David J. Sullivan, MD

Acknowledgements

First and most deservedly, I'd like to thank Dr. Gary Ketner, who has been a true mentor, not only guiding every aspect of the research but also life outside of the lab. From the first sit-down meeting to the approval of this thesis, he has shown me nothing but respect and interest in every question, idea or comment, however silly. I hope to follow his example and gain the respect not only from the field of science but from those around me. I also want to acknowledge the line of predecessors on the VIP project, Cailin Deal who took the first step in VIP against malaria, Renuka Joseph and Brendan Dolan who has succeeded in proving the possibility of VIP over and over again. I'd also like to thank Gloria Shin, who has helped me settle in the lab and taught me all the tips in working in the lab.

I would also like to thank the persons who were much invested in me and the experiments: Mary Archer and Casey Kissell for teaching me how to handle mice and Aotus from day 1, and accommodating all the procedures in and out of the animal facility, Jessica Herrod and Jacqueline Brockhurst for the current and future experiments with the Aotus monkeys, Abhai Tripiathi and Godfree Mlambo for culturing and preparing parasites and mosquitoes for the Aotus monkeys and mice, Christopher Kizito for all procedures with mice and Aotus in the insectary, Melanie Shears for teaching me how to dissect mosquitoes, Gibbs Nasir for helping me choose MMI and also showing me how to dissect mosquitoes and Jane Xie for experiment consultation. Though I have riddled the persons listed above with questions, I'd like to thank Yevel Flores-Garcia especially, who I have constantly chased and has provided invaluable guidance and advice in experimental procedures.

Thank you, Dr. David Sullivan, for being the main advisor for the Aotus project from design to actual experiments, and for serving as the secondary reader for my thesis. I'd also like to thank Kristin Poti for parasite detection in the Aotus monkeys.

I would also like to thank Dr. Prakash Srinivasan for engaging in thoughtful discussions and helping me to think critically of the experiments and Shuhao Xiao lab for AAV experiment cooperation.

I also want to thank my parents, who has sacrificed the most and given so much for me to be here, and Sanghee Song, who has supported me in every decision, whether it be a mice infested or ceiling-less apartment, and who always found a way to make me feel loved. Also, my son June, who has never failed to make things hard but also never failed to make me smile.

Lastly, but most importantly, I thank God for the opportunity to be in this academically rigorous and supportive institution and giving me the strength to finish my degree.

Table of Contents

List of Tables

List of Figures

Introduction

Burden of Malaria and Human Malaria Lifecycle

Malaria is a severe febrile illness caused by genus *Plasmodium* parasites with symptoms that range from fever, splenomegaly and anaemia to cerebral malaria and death [1]. The parasite is transmitted from person/animal to person by female *Anopheles* mosquitoes [1]. Though different methods of interventions are employed every year, the burden still persists and in 2017, 219 million cases were reported, with 435,00 deaths [1]. Of those, 92% of the malaria cases and 93% of deaths occurred in WHO African Region, 61% of the deaths occurring in children under 5 years [1]. The pathogen also incurs economic burden, as an estimated $3.1 billion was spent in 2017 by endemic governments and international partners in an effort to alleviate the disease burden [1].

The malaria affected regions rely mainly on the anti-malarial drugs such as chloroquine and artemisinin-based combination therapies, and vector control methods. However, recent reports have documented parasites resistant to quinolines and artemisinin-based drugs, and vectors that are resistant to insecticide treatments [2, 3]. With the trend of diminished decline of malarial burden with increasing funds used on current prevention / treatment methods [4] and reports of resistance in anti-malarial drug and vector control methods, the need for a new intervention such as vaccines or prophylaxis is evident.

Plasmodium falciparum lifecycle within the host and rationale for pre-erythrocytic stage vaccine

The genus *Plasmodium* is a single-celled parasite known to infect different organisms including reptiles, birds and mammals and notably, humans [5]. Five

Plasmodium species have been identified to infect humans, *P.malariae, P.ovale, P.vivax, P.knowlesi* and *P.falciparum* [5]. Species *P. falciparum* has been identified as the largest portion of the burden, and is responsible for febrile Malaria in 99.7% in WHO African Region, 62.8% in Southeast Asia, 69% in Eastern Mediterranean and 74.1% in WHO Americas [4].

The *P.falciparum* has a multi-stage complex lifecycle in the vertebrate host as well as the vector host. It changes into many morphologic forms that allow the parasite to carry out its appropriate task in a specific stage of infection. From the vector mosquito's salivary gland, the sporozoite form enters the dermis lingers at the site of injection for about 1-3 hours [6-8]. The sporozoite is in constant state of movement, and its gliding movements and Trap-Like Protein (TLP) allow for penetration from dermis into the blood vessel. While circulating in the blood, sporozoite crosses the sinusoidal barrier in the liver using the sporozoite microneme protein essential for transversal (SPECT), SPECT2 or also known as perforin-like protein-1, cell transversal protein for ookinetes and sporozoites (CelTOS), Phospholipase (PL) and gamete egress and sporozoite traversal protein (GEST) [9]. Upon interaction with the hepatocytes, the sporozoite 'switches' from migratory mode into invasive mode. Upon contact with the hepatocytes, the thrombospondin-related anonymous protein (TRAP), apical membrane antigen-1 (AMA-1) protein and circumsporozoite (CS) protein work in collaboration permit the parasite to enter the cell. Within the liver, or the exo-erythrocytic form, the parasite replicates and in 2-10 days, up to 40,000 merozoites erupt from each hepatocyte and enter the bloodstream [9].

In the erythrocytic stage, the released merozoites attach themselves to erythrocytes by forming a tight junction through AMA-1 and RON complex and efficiently enters the cell through sequence of lipid-rich rhoptry contents and actomyosin motor. The pore created by the entry is sealed subsequently by the fusion of membranes in the posterior end of the merozoites [9, 10]. Within the erythrocyte, the merozoite undergoes replication (schizogony) and in 48 hours, it ruptures the cell releasing 16-32 merozoites into the blood stream for further infection [9]. Some of the released merozoites can develop into male (microgamete) or female (macrogamete) form of gametocyte, the sexual stage of malaria [9]. The sexual maturation of the gametocytes takes about 11 days, in which time, they are sequestered within the bone marrow to avoid the clearance by the spleen and the host immune system [9]. The mature gametocytes then are taken up by the female *Anopheles* mosquito vector in the peripheral circulation and fuse to form a zygote and subsequent genesis of sporozoites to restart the replication in a host [9].

Vaccination efforts have mainly focused on pre-erythrocytic stage vaccines targeting prevention of sporozoite invasion into hepatocytes and replication within liver stage and erythrocytic stage vaccines against asexual merozoites [11, 12]. Although intervention in each stage is beneficial to the host, immune responses against the pre-erythrocytic and sporozoite form is most advantageous because it prevents the overall infection in the host, as well as replication and transmission of the parasite [13]. Additionally, investigations on mosquito sporozoite injection showed that as few as 20-120 sporozoites were injected into the dermis [14] and of those, at least 20% were drained into the proximal lymph nodes where they are degraded subsequently [6, 15].

This suggests that there is a bottleneck effect at the site of dermal inoculation [7] that could potentially provide the most efficient intervention at the pre-erythrocytic stage, given that the sporozoite also lingers at the site of injection between 1-3 hours [6]

Investigations of vaccination using sporozoite was first exploited against murine malaria *Plasmodium berghei* that was attenuated through x-ray radiation of the mosquito vector, which was successful in inducing humoral immune response that was able to neutralize the invasion of sporozoites [16]. The same attenuated sporozoite vaccination strategy was applied to the human malaria species *P. falciparum*, and showed proof-of-concept of sterile immunity through humoral immune response against the pre-erythrocytic stage of the parasite [17].

However, as general consensus that natural infection does provide partial protection but not sterile immunity, and the immune response was much dependent on age and dose-dependent [11], different antigens in the pre-erythrocytic stage has been targeted to elicit a more robust and specific immune response. Antigens that have been identified as a potential target include antigens that are involved in the sporozoite motility, such as CelTOS antigen expressed in the motile stage of the sporozoite and ookinete [18] and Thrombospondin-related adhesive protein (TRAP) protein that is highly involved in enabling motility from the skin into the hepatocytes [19-22] and Liver Stage Antigen-1 (LSA-1) antigens that are expressed on the early stages of infection in hepatocytes unique to the *P.falciparum* species [23]. Preliminary studies have already shown that motility targeted antigens and liver stage antigens have been successful in eliciting partial protection [24-26].

Of the antigens under scrutiny, repeatedly the most well described and immunodominant antigen is the circumsporozoite protein (CSP) [13]. CSP antigen was identified as an antigen in both human and rodent malaria sporozoites [27] and antibodies directed against the CSP has been identified to have the highest affinity towards the sporozoite in an competitive assay [28]. Antibodies directed against the CSP antigen has been suggested to affect the sporozoite's motility, shown from the differences in net displacement in the presence of the anti-CSP antibodies [7]. Specifically, the most immunodominant epitope in the CSP has been identified as the NANP repeat region [13] which is also conserved throughout the *P.falciparum* species around the world [13, 29], and have been branded as an ideal target for vaccine development [13].

CSP and RTS,S/AS01

CSP is the most abundant surface protein on the sporozoite. From the sporozoite surface, the CS is composed of glycosylphosphatidylinositol (GPI) signal, TSR domain, the C-terminus, the central repeat region, Region 1, and the N-terminus [30]. It is highly sought after in the quest for vaccines as immunodominant response is elicited against the repeat region of the CSP [13]. The CSP is highly relevant in the invasion of sporozoite from the site of injection into the hepatocyte as the CSP undergo conformational change in different phases [31, 32]. In the migratory phase of the sporozoite, the N-terminus masks the adhesive C-terminal domain and upon contact with a hepatocyte, it changes its conformation to invasion phase, where the C-terminal cell-adhesive domain is exposed. It is the proteolytic cleavage of CSP occurs in the highly conserved region I by the papain

family cysteine protease that converts from the CSP migratory to invasion phase, and it has been suggested that CSP is essential in invasion into the hepatocyte [31, 32].

RTS,S/AS01, the vaccine in the most advanced stages of the clinical trial uses a portion of the CSP in its formulation [33]. Specifically, RTS,S is a two part vaccine where the C-terminal half of the CSP fused to the hepatitis B virus surface antigen (HBsAg) is expressed into virus-like particles (VLP) that display CSP and HBsAg on its surface. In addition, the CSP and HBsAg (RTS) is expressed with pure HBsAg (S) formulation in 1:4 ratio [34]. The antigens are expressed from genetically engineered *Saccharomyces cerevisiae* yeast cells and its novel adjuvant systems AS01 was developed to elicit a more robust and longer-lasting immune response [34].

In a phase 2a clinical trial, 50% of the vaccinees were protected and the anti-CS titer rose to a high level. Anti-CS antibody was a correlate of protection, as protected individuals had over 2-fold titers than the unprotected individuals [35]. Encouraged by the data, the vaccine was used in an endemic population for the phase 3 clinical trial in children 5-17 of age, followed up to 7 years for vaccine efficacy. In relative similarity to phase 2 clinical trial, in the first year of the trial, the efficacy of the vaccine was 35.9% (8.1-55.3%, 95%CI) [36]. However, the efficacy after 7 years declined to just 3.6% (-29.5-28.2, 95%CI), and negative efficacy was observed in the 5th year of surveillance [36]. Investigations into the clinical trial lead to a few conclusions, including the mismatched strain of *P.falciparum* in the area [37], minimal T-cell immune response, and the endemicity of the population where the semi-immune status of the endemic population that may have worked adversely and prevented full immune response against the vaccine [11].

Though RTS,S/AS01 has been licensed by the European Medicines Agency (EMA), lessons from the RTS,S/AS01 have encouraged research in different forms of CSP vaccine candidates, such as R21, identical in RTS,S construct but increased ratio of the CSP-HBsAg to HBsAg (S). The basis of the vaccine is to concentrate on increasing the anti-CSP antibody with a higher ratio of RTS,S at lower overall dose and have entered phase 1/2a clinical trials [38].

Some of the main emphasis from the RTS,S/AS01 clinical trials was waning in vaccine efficacy/immune response and antibody-mediated protection [36]. From the RTS,S/AS01 phase 3 randomized trial, the protective immunity was correlated with presence and level of antibody against sporozoites [39, 40]. Though statistical evidence model provides that combined antibody and cell-mediated immune response provide better fit to protection, (Immune response of antibody alone estimated 32% protection (24-41% CI 95%) and 40% with CSP-specific CD4+ T-cell response) [39] the presence of neutralizing antibodies alone provided the major correlate of protection [39]. This conclusion is not surprising however, as past experiments using sera from humans and animals vaccinated with attenuated sporozoite have shown that anti-CS antibodies could neutralize and inhibit sporozoite and its invasion in vitro and in vivo [13, 41, 42]. As CSP is heavily involved in motile and invasion function of the sporozoite and the proteolytic cleavage site is close to the NANP central repeat antibody-binding sites, some of the monoclonal antibodies (mAbs) have been identified to interfere with the functions of the CSP and inhibit sporozoite infection [43].

Though passive transfer of antibodies is the most efficient method of prevention of infection and transmission [44], and would be a valuable asset in combating malaria,

the duration of its half-life, production line, delivery system and logistical hindrance is a big obstacle for use in malaria endemic areas. However, an alternative method of antibody transfer in recombinant Adeno-associated Virus sheds a light in innovative method of delivering mAbs.

Adeno-associated Viruses

Adeno-associated Virus (AAV) is a Dependoparvovirus in the family of Parvoviridae [45, 46]. It is an unenveloped DNA virus with a icosahedral capsid about 26nm in size [46]. The virus capsid is composed of capsid protein VP1-3, in 1:1:10 ratio – totaling 60 proteins per virus particle [45]. Its genome is about 5kb and can carry plus or minus sense single stranded DNA viral genome [45]. The DNA genome is flanked by inverted terminal repeats (ITR) that form a T-shape secondary structure and contains the origins of replication and packaging signal [45, 46]. The DNA genome only has two open reading frames, the rep and cap genes. Rep encodes 4 replication genes rep78, rep68, rep52, rep40 and cap encodes VP1-3 and Assembly Activating Protein (AAP) that promote virion assembly [46, 47]. These proteins are translated through alternative splicing and use different initiation codons [45, 46]. As the name suggests the virus depends on adenovirus or herpesvirus for essential proteins and molecules for replication, assembly and egress [45, 46].

AAVs are founds in multiple vertebrates including humans. Human AAVs are closely related to primate AAVs [45]. AAVR (KIAA0319L) protein is an receptor protein for multiple serotypes of AAV [48-50] and has also been characterized as a facilitator in intracellular trafficking [50]. The virus is internalized through endocytosis

[51], and pH dependent structural changes and viral DNA is released into the nucleus [52] by the use of cytoskeletal network [53]. Generally, the AAVs are not known to cause human diseases although there is a low tendency for the virus genome to integrate itself into a AAVS1 site in chromosome 19 to establish a latent form [54].

Recombinant AAVs or rAAVs are AAVs that have the exact same capsid but carry a therapeutic expression cassette in place of the of its rep and cap genes [45]. The only conserved viral genome is the ITR that is essential for virus replication and assembly during transfection for vector production [45]. The virus replication cycle enables complete replacement of the genome (up to 5kb [55] and allows for expression of foreign genes in infected cells. Widely used serotypes for rAAVs have been well characterized in receptor recognition, as receptors such as glycoproteins dictate its tissue and cell tropism[45]. After the transgene has been released into the nucleus by endocytosis, the double strand forms a circular rAAV intermediates that remain as an episome and allow long-term transgene expression [56]. This is one of the rate-limiting steps in transgene expression because the virus must complement its DNA with a leading/second strand synthesis [57, 58]. To eliminate the rate limiting step, single-chain AAV or scAAV are made to skip the DNA strand synthesis [59] and higher yield of the expression of the transgene. However, the high yield comes at a cost as the scAAVs can only accommodate half the transgene size[45, 59].

The first ever rAAV product licensed is Glybera, alipogene tiparvovec, that is used as a gene replacement for treating lipoprotein lipase deficiency [60]. The first rAAV product licensed in the US is Luxturna (Voretigene neparvovec-rzyl) that is used also as a gene replacement for defective RPE65 gene [61]. Different rAAV strategies exist,

including gene-silencing for monogenic toxicity genes, gene-editing using CRISPR-Cas or Zinc-finger nuclease technology and gene-addition for expressing higher concentration of molecules for chemical imbalance, or for prevention of infectious diseases.

rAAV VIP and Anti-CSP monoclonal antibodies (mAbs)

From clinical trials of RTS,S/AS01 and vaccinations with irradiated sporozoites in animal and human model, it was evident that antibody against the sporozoite / CSP was the most accurate correlate of protection [39, 40] and that traditional vaccines had a limited efficiency over the longer periods due to waning immunity [36]. As an innovative and possible alternative against observed immune response from traditional vaccines, rAAV has been engineered to express antibody transgenes in infected cells [62-67].

The transduction of antibody transgene is termed vectored immunoprophylaxis (VIP) and the VIP system is aimed to express antigen specific mAbs for an extended period to prevent infection or intervene further infection[62]. The VIP system uses wtAAV derived plasmid backbone, however, the ITR region is the only remaining viral DNA viral gene having been replaced by optimized genes for efficient mAb gene expression, including cell-specific promoter, poly-adenylation signal, and post-transcriptional enhancer [62, 65, 66] (Fig. 1). The rAAV-VIP system has been tested against epitopes on various pathogens and has provided sterile immunity through its antibody expression, including broadly neutralizing antibodies (bnAbs) against gp-120 on HIV-1 [62, 64, 67], hemagglutinin on influenza[63] and CSP (NANP repeat). on the sporozoite stage of *P.falciparum* [65].

In rAAV-VIP system against CS surface protein on the sporozoite stage of *P.falciparum,* antibodies 2A10 and 2C11 [28], were expressed in murine model [65]. The expression levels were dependent on the virus genome copies (GC) injected intramuscularly and mAbs concentration over 1000ug/mL were observed after 4 weeks. Protective immunity from mosquito delivered sporozoites was observed in 60% of the rAAV expressing 2A10 mAbs, and 30% of the mice expressing 2C11 mAbs. In accordance with antibody levels as correlate of protection observed from clinical trials, mice expressing high level of 2A10 mAbs (>1000ug/mL) had 100% protection rate, while lower level of mAbs expression showed varying level of protection [65].

Clinical trials of human immunization with irradiated *P.falciparum* sporozoites has yielded in multiple potent antibodies that also target the CSP in the sporozoite stage of the human malaria [68, 69]. mAbs named CIS43 isolated from protected individuals provided the highest protective effect against the liver-stage parasite burden in mice, and also showed the highest level of protection than even previously mentioned 2A10[68]. It was most notable in that though the antibody titer was lower in mice with CIS43 than in mice with 2A10, higher level of protection was observed in mice with CIS43 [68]. MGU-12 was also isolated from CHIM, and in murine model, it also showed high protective effect in liver-stage burden [69]. While the two isolated antibodies are impressive in that they show highly protective effect against sporozoite challenges, it is most intriguing that the binding site for these antibodies are at the “junctional epitope” between the N-terminus and central repeat region, diverging from the immunodominant central NANP repeat region, a region that is not included in the RTS,S/AS01 formulation. In this thesis, we report the expression and protective efficacy of rAAV of newly described CSP-

directed antibodies and analyze the vector and VIP expression kinetics. The protective efficacy of new antibody expressing rAAV are tested in murine model as to compare with formerly analyzed 2A10 mAbs [65].

In addition, the formerly described rAAV-VIP system of 2A10 mAbs will be translated into nonhuman primate model in an effort to more accurately observe expression kinetics and protective efficacy in an animal model resembling human immune system and address possible safety issues. The rAAV expression and malaria-mosquito challenge will be conducted on *Aotus nancymae* monkeys that can uniquely be infected by human *P.falciparum*[70, 71] and are an accurate portrayal for human response against malaria infections and vaccines [72].

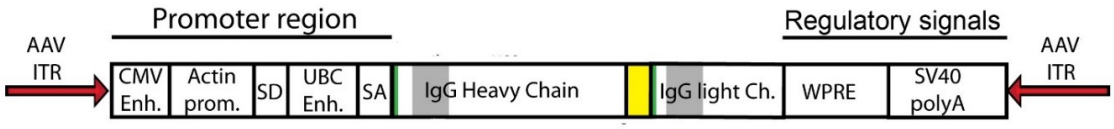

Figure 1. VIP Modular expression cassette

Red arrows: AAV inverted terminal repetition sequences containing AAV replication and packaging signals for vector production. **Gray rectangles**: IgG variable regions. These are flanked by unique restriction sites (not shown) to facilitate replacement to generate antibody genes with new specificities. **Yellow rectangle:** Self-cleaving peptide that cleaves the primary translation product into native heavy and light chains. **Green bars:** export signal sequence. The remaining elements, WPRE, SD, SA etc., are regulatory sequences that drive efficient mAb gene expression in cells.

Materials and Methods

Vector Plasmid Construct and Cloning

The published 2A10 (anti-CSP NANP repeat region) and b12 (anti-HIV-1 gp120 protein) DNA sequences were cloned into the VIP expression cassette by Dr. David Baltimore's Laboratory at California Institute of Technology [62] and its protective efficacy against HIV-1 and *P. falciparum* parasites were previously tested by the Baltimore Laboratory [62] and our laboratory [65] respectively. In this thesis, b12 antibody was used as a negative control and 2A10 was used as a positive control antibody with a repeated and stable protective rate [65].

As described, the monoclonal CIS43 and MGU12 antibodies both specifically bind to the junctional region of the CSP between the N-terminal peptides and NANP peptide repeat region. CIS43 binds to an epitope 15-mer N'-NPDPNANPNVDPNAN-C' (Peptide 21) (Fig. 2) and MGU12 binds to 15-mer N'-KQPADGNPDPNANPN-C' (NPDP15) (Fig. 3)

To clone the variable regions (referred to as inserts) of the two antibodies into the existing 2A10 VIP vector the published Heavy (V_H) and Kappa (V_K) inserts were first synthesized by Thermo Fisher Invitrogen GeneArt Gene Synthesis. Endonuclease restriction sites NotI and AgeI flanked V_H and NsiI and PstI flanked V_K for 2A10 VIP vector, and the GeneArt CIS43 and MGU12 heavy and kappa inserts were also flanked with the respective endonuclease restriction sites.

For CIS43 cloning into VIP vector, 5ug of GeneArt CIS43 and 2A10 VIP plasmid DNA were separately incubated with NotI and AgeI each for V_H region. The mixture was

incubated at 37°C for 4 hours. After incubation, the mixture was ethanol precipitated. The ethanol precipitation steps are: 1) addition of 2.5X volume of 100% EtOH 2) place on ice for 15 minutes 3) centrifuge for 15 minutes at 14,000rpm 4) aspirate the supernatant 5) dry the precipitate for 15 minutes, and 6) add desired final volume of TE.

Both digested plasmids were mixed with 6X Blue Gel Loading Dye (NEB) and loaded on to a 1% agarose gel containing 0.5ug/mL ethidium bromide and 0.5ug/mL ethidium bromide TE running buffer at 50mA alongside a 1kb Plus Ladder (NEB). The VIP vector (minus the 2A10 V_H insert) and CIS43 V_H insert were separated by the gel and were subsequently extracted from agarose gel using QiAquick Gel Extraction Kit (Qiagen) and saved for the ligation reaction. The extracted linear DNA concentration was measured at 260nm wavelength. To ligate the VIP vector and CIS43 V_H insert, the plasmids were added at a 1:1 molar ratio with DNA Ligase I. The mixture was incubated at 37°C for 4 hours.

Bacterial transformation was conducted with DH5-alpha cells (Subcloning DH5-a competent cells by Thermo Fisher Scientfic) according to manufacturer's instructions. The transformed DH5-a were plated in 60 ug/mL ampicillin Agar and incubated at 37°C overnight to screen for the VIP plasmid transformed isolates which contain ampicillin resistance gene.

Isolates of transformed cells were grown in in Luria Broth at 37°C overnight, and Qiagen Mini/Midi Kit (Qiagen) was used to extract pDNA and its concentration was measured with nanodrop at 260nm wavelength.

To confirm the ligation of CIS43 V_H variable region into the VIP vector, endonuclease reaction with *DraIII* was conducted to determine the presence of the restriction sites that could differentiate between the 2A10 and CIS43 variable regions (Fig. 5A). The cloning procedure for the second variable site, V_K, did not yield in a viable copy, therefore NEB Builder Gibson Assembly Kit (New England BioLabs) was used to for V_K cloning. Once the ligation of both CIS43-V_H and V_K was confirmed by *DraIII* and *KpnI* endonuclease activity unique to CIS43 V_H and V_K, (Fig. 5B) the plasmid was sequenced by Johns Hopkins Sequencing Core for further confirmation

For the MGU12 construct, both of the variable regions were cleaved and ligated simultaneously using the NEB Builder Gibson Assembly Kit (New England BioLabs). The MGU-12 construct was also transformed into DH5-a cells, screened by ampicillin resistance, its DNA extracted by Qiagen Mini/Midi Kit (Qiagen) and sequenced at Johns Hopkins Sequencing Core to confirm the MGU-12-VIP plasmid.

Comparative Functionality of CIS43 and MGU12 Vector Plasmid

To assess the functionality and measure the antibody expression levels of the CIS43 and MGU12 VIP construct, the VIP plasmids were transfected in 293T cells, and antibody titers were measured by ELISA against hIgG and rCSP. 2A10 VIP plasmids with known functionality and levels of expression in *vitro* and in *vivo*, were transfected as a comparison.

For plasmid transfection, 300,000 HEK-293T cells were plated 48h prior to plasmid transfection to achieve 75% confluency in a 6-well plate. The cells were grown

in Dulbecco's Minimum Essential Media (DMEM). Two hours prior to plasmid transfection, the media was changed to D10 (DMEM containing 10% Fetal Bovine Serum, 1% Penicillin/Streptomycin, and 1% L-glutamine)

Appropriate volume for 2ug of DNA and 3uL of BioT (Bioland Scientific LLC) were mixed with 100ul of serum-free DMEM, centrifuged briefly and incubated at room temperature for five minutes. The mixture was then added to each well plate, and gently stirred. 100uL samples were collected 24 hours and 48 hours post transfection and quantified for human IgG by ELISA as described [62].

rAAV Production and Purification

Three days prior to AAV plasmid transfection, $3.75x10^6$ HEK 293T cells were plated in Nuclon Delta Surface 15cm plates (Thermo Scientific) with D10 media. 2 hours pre-transfection, the media was replaced on the 15cm plate with fresh D10. In a 50ml Centrifuge Tube (Corning), 24.6ug of AAV VIP plasmids (2A10, CIS43, MGU-12 or b12), 98.4ug of pHELP helper plasmid (Applied Viromics LLC), and 197ug of AAV plasmid that contains replication genes from AAV2 and capsid gene of AAV8 (AAV2/8), and 240uL of BioT(Bioland Scientific LLC) were mixed with 16ml of DMEM and incubated at room temperature for 5 minutes (Fig.4). The ~16mL of pDNA and BioT were separated into 15cm plates.

The media culture containing the virus was collected at 36, 48, 72, 96, 120 hours post transfection and filtered through a 0.22um PES Membrane Stericup Quick Release (Millipore). The supernatant was saved in 4C cold room for virus purification. 100uL of

supernatant was set aside to assess virus production at each timepoint. ¼ volume of 5X Polyethylene Glycol (Promega) was added to the virus supernatant and allowed to precipitate overnight.

The PEG precipitated virus was divided into two and centrifuged (Sorvall RC5C Centrifuge) at 5000rpm for 30 minutes, and the supernatant was discarded. Each tube of virus was resuspended in 5ml of Cesium Chloride (Research Products International) solution of 1.37g/mL density. The virus in Cesium Chloride (CsCl) solution was combined with additional 10ml of CsCl solution, a total of 20mL. The virus was then equally distributed into Quick-Seal Ultracrimp Tubes 11.5mL (Thermo Scientific) with Pasteur pipettes. Additional CsCl solution was added up to the neck to completely rid of bubbles. The Quick-Seal Ultracrimp Tubes were then sealed with cap and sealer (Thermo Scientific). The tubes were placed in Sorvall WX Ultra Series (Thermo Fisher Scientific) and spun in an ultracentrifuge at 60k, 20'C, for 20+ hours.

The Quick-Seal tubes were recovered from the ultracentrifuge and clamped onto a stand. 20G needles were used to pierce through the center of the bottom curvature and removed. Below the neck of the Quick-seal tubes were pierced with 27G needles and the butt-end was blocked with a finger to stop the flow of the tube content. To collect the flow-through from the bottom of the tube with a 96-well plate, the 27G needle was manually controlled to allow constant drip of the CsCl mixture solution. Each well was then checked for density through a refractometer and recorded. Because the properties of AAV particles are known, wells that were $1.3755 > X > 1.3655$ on the refractometer index range were pooled for the dialysis step.

For dialysis of the rAAV, the CsCl solutions from the 96 plate wells were transferred into the Amicon Ultra (Merck Millipore) filter tubes. Additional TFB2 was added to fill up to 15ml in the Amicon filter tube, and the mixture was centrifuged for 3000 rpm, 4C for 1 hour. The flow-through was centrifuged for about 1 hour or until the liquid in the filter was less than 1ml. The flow-though was discarded and additional TFB2 was added to the filter up to 15ml. The TFB2 and centrifuge was repeated three times until the retentate was less than 500uL. The retentate was then used to rinse the filter on the Amicon Ultra filter tube to and all the retentate was collected and frozen at -80'C.

rAAV Quantification

AAV quantification was conducted as described previously [62] using PCR. The sample rAAV and the standard (AAV8 expressing b12 mAb with the concentration of $1x10^{12}$ GC/mL) were both diluted 10-fold in DNAse/DNAse buffer and incubated at 37°C for 30min. For the negative control, instead of the sample, DEPC treated water was added(Promega) and incubated. 7 dilutions were made for the standard which was diluted 4-fold with DEPC treated nuclease free water(Promega). The sample rAAV was diluted three times, a 100 fold and two subsequent 10 folds. The negative control was not diluted.

The PCR mastermix composed of 78.75% CYBR-Green PCR Mastermix (Thermo Fisher), 19.95% DEPC treated nuclease free water, 3.15% forward and 3.15% reverse CMV promoter primers (5′ CMV: AACGCCAATAGGGACTTTCC and 3′ CMV: GGGCGTACTTGGCATATGAT). 10uL of the master mix and 5uL of either standard, negative control or rAAV sample was loaded onto MicroAmp Fast Optical 96-well Reaction Plate (Thermo Fisher). Each sample was quantified using qPCR (Applied

Biosystems One Step Plus qPCR) with the following program: 1X 50°C for 2 minutes, 1X 95°C for 10 minutes and 60X of 95°C for 15 seconds and 60°C for 60 seconds.

Mouse rAAV injection and serum collection

Quantified recombinant viruses were thawed and diluted with TFB2 to achieve $1x10^{11}$ genome copies (GC) or $3x10^{11}$ GC in 100uL volume. 1/2cc Insulin syringes (BD) were used to inject 50uL of TFB2 diluted viruses into gastrocnemius muscle (i.m.) in each hind leg. 4-6 week old female C57BL6 mice were used in groups of 10 with different recombinant AAV. Post i.m. injections, blood was drawn at different time points through cheek-bleeds. Sera was separated by BD Microtainer SST (BD) tubes at 5,000rpm for 10 minutes, and stored at -80°C.

Aotus rAAV injection and serum collection

Quantified recombinant viruses were thawed and diluted with TFB2 to achieve $1x10^{13}$ genome copies in 200uL volume. 1ml TB Syringes (BD) were used to inject TFB2 diluted viruses at 6 different sites in the quadricep muscles, 3 sites on each quadricep muscle. Details of all *Aotus* nancymae monkeys that were included in the protocol are listed in Table 1. Post i.m. injections, blood was drawn at different time points (Table 2) through either femoral vein or great saphenous vein bleeds. Sera was separated in 1.5mL FLEX TUBE (Eppendorf) at 7000rpm for 5 minutes and stored at -80°C.

Quantification of Monoclonal antibodies by ELISA

Quantification of human anti-CSP antibodies are conducted as previously described (Deal 2014). Each well of the 96-well ELISA plate (2HB Immunlon Flat Bottom Microtiter plate) was coated with 100µL of rCSP purified from MR-272 at 0.5ug/mL in PBS overnight at 4°C. The unattached rCSP was washed away with 200uL of PBS-Tween three times, and 200uL of PBS three times. 10% FBS, 0.05% Tween PBS solution was used as a block and incubated at 4°C overnight. The plate was again washed with PBS-T and PBS. In 96X Serocluster Plates (Costar), sera were diluted in the blocking solution starting at 1:1500 and diluted by 3-fold. 100uL of the diluted sample sera were then transferred to the ELISA plate and incubated at room temperature (RT) for 1 hour. Followed by another 3X wash with both PBS-T and PBS, 100uL of Human Kappa light chain antibody (Bethyl A80-115P) diluted by the blocking solution in 1:10,000 was added and incubated at RT for 1 hour. The ELISA plate was washed for the last time with PBS-T and PBS and 100uL of BD OptEIA TMB substrate reagent mixture was added and incubated at RT for 15 minutes, in the dark. After 15 minutes, 100µL of 4N sulfuric acid was added to halt the of substrate-enzyme reaction. ELISA plates were measured by Multiskan MCC (Thermo Fisher Scientific) plate reader with Accent Software for Multiskan (Thermo Fisher Scientific) at 450nm wavelength. The human anti-CSP antibodies in the *Aotus* sera were detected with an identical protocol.

Transgenic *P.berghei*/*P.falciparum* Challenge in Mice

Mice were challenged with transgenic murine malaria, *P.berghei*, expressing *P.falciparum* CSP (*Pb/Pf*CSP Nardin strain) that was provided by the Zavala laboratory.

The Johns Hopkins Parasite Core provided the *Pb/Pf* Nardin strain infected *Anopheles stephensii* mosquitoes for challenge. The transgenic parasite challenge was conducted with mosquitoes that were 21-24 days post blood feed.

Prior to the malaria parasite challenge, 15-20 *Pb/Pf* Nardin strain infected A. *stephensii* mosquitoes were temporarily knocked out in the -20, placed in the ethanol and transferred to PBS. The mosquitoes' salivary glands be dissected under the microscope with 26G PrecisionGlide Needle (BD) and were checked for the presence of parasites under the microscope. The challenge was only conducted if the rate of sporozoite infectivity of the salivary gland was over 80%. The day prior to the challenge, 8-12 infected mosquitoes were separated into each paper cup with open netting on the top for each mouse. The infected mosquitoes were starved overnight and were dehydrated 4 hours prior to the challenge.

In order to preserve natural route of infection, each mouse was placed on a paper cup netting after anesthetization with 100-120uL of Ketamine that was given intraperitoneally. The mice were placed on the paper cup netting for base 10 minutes with occasional blow of CO2. After the feed on the mice, the infected mosquitoes in each paper cup was knocked down, killed in 70% ethanol and its midgut was dissected to determine the number of mosquitoes that fed on each mouse.

To determine days to patency, starting from day 4 post mosquito feed, blood smears were made from tail bleeds to observe level of parasitemia. The blood smears were fixed on glass slides by methanol and stained with 10% Giemsa stain (Sigma-Aldrich) for 30 minutes. The blood smear was observed under the 100X oil-emulsion

microscope. After 2 days of confirmation of parasitemia, the mice were euthanized. Protection from infection was determined if no infection was observed past day 14.

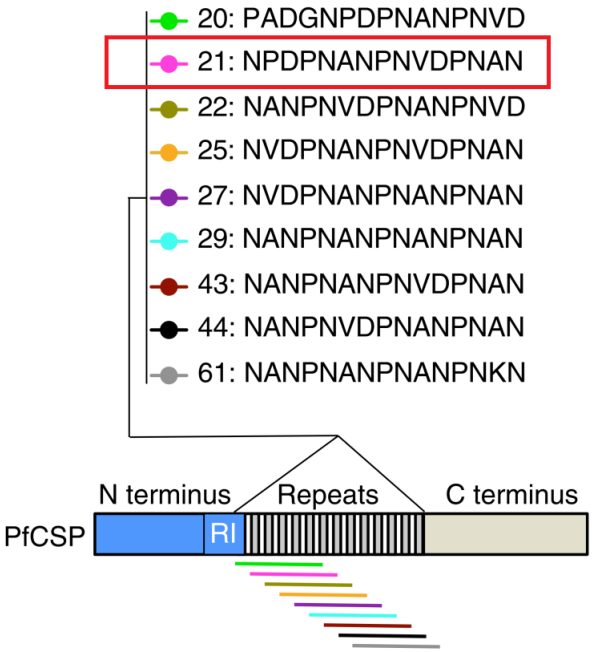

Figure 2. The recognition site of mAb CIS43 analyzed by Tan et al.

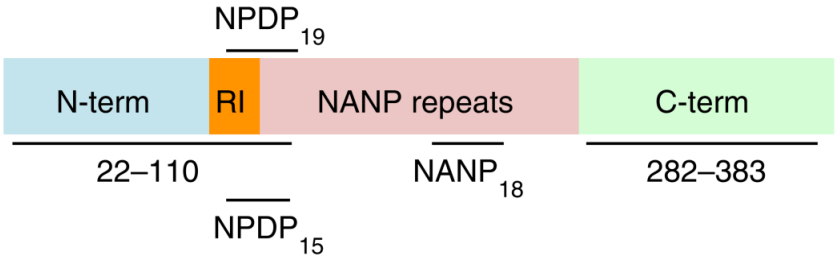

Figure 3. The recognition site of mAb MGU-12 analyzed by Tan et al.

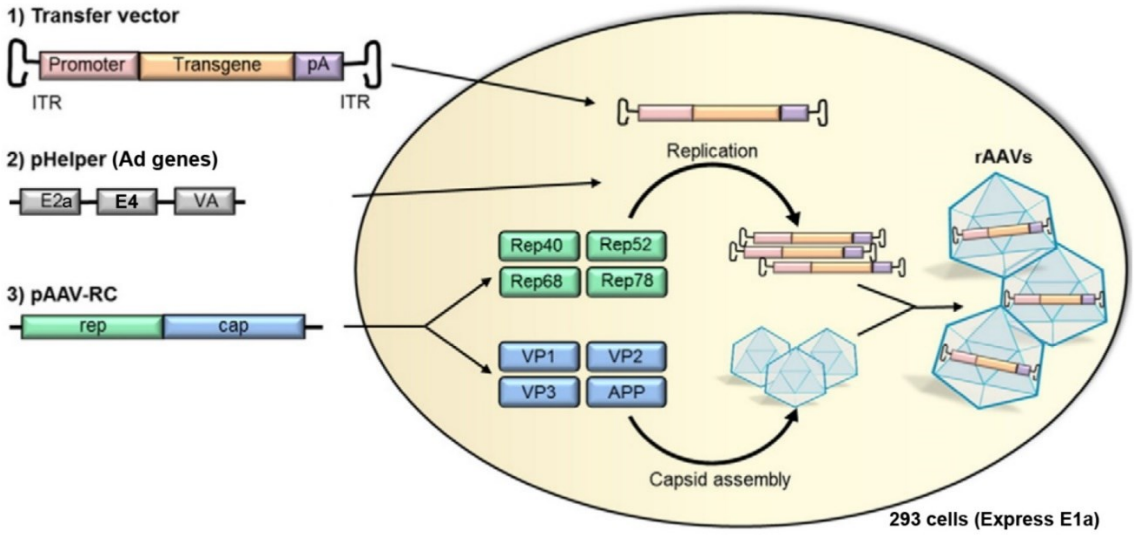

Figure 4. AAV Transfection Scheme taken from Saraiva et al. [73]

The transfer vector (VIP), pHELP, and pAAV plasmids are transfected in a 293 cells that express the E1a gene. The VIP is replicated and are encapsidated in the AAV capsid that have been translated by pHELP and pAAV. The newly formed rAAVs are purified through CsCl gradients and stored at -80˚C.

Results

Though RTS,S/AS01, the first malaria vaccine, did not provide a high protective efficacy in areas of endemicity [36] it has provided valuable information on antigen exposure in naïve population and semi-immune population that elicit different immune responses [11]. It also provided additional evidence on the major correlate of protection, the presence of the antibody as the biggest factor in prevention of malaria infection [36].

The VIP system provides the possibility of alternative method in providing proven antibodies that neutralize the pathogen [62-65, 67]. In a study that used the rAAV-VIP system to deliver CSP- binding and sporozoite neutralizing 2A10 and 2C11 antibodies, the antibodies were able to provide sterile immunity in 60% of the mice, and the protective efficacy was reflective of antibody level expressed by the VIP system. Because the expression kinetics of the antibody are a major factor in achieving sterile immunity, investigations into further VIP-antibody pairing could provide invaluable information on the VIP system and ideal candidates for the most efficient antibody delivery.

In our experiments, we have cloned the newly described CIS43 and MGU-12 V_H and V_K inserts into the existing VIP plasmid that have 2A10 V_H and V_K inserts. The CIS43, MGU-12 as well as existing 2A10 and b12 VIP plasmids were evaluated by expression assay *in vitro*, encoded in rAAV2/8 vector and transduced in mice. The expression of each VIP was evaluated by conducting ELISA to detect human monoclonal antibodies with anti-CSP activity. In the ELISA, the sera are diluted 3-fold starting from 1:1500 to 1:3,280,500. A sample's dilution was considered 'positive' if the optical density value was 2X the amount of background signal. By recording the highest dilution

of sample that was considered 'positive' each week, we were able to see the VIP expression kinetics throughout an 8-week period and compare them within different VIP expressions.

After week 8, all mice were challenged by bites from *Anopheles stephensii* mosquitoes infected with transgenic *Pb/Pf*CSP parasites. Parasitemia was confirmed by blood smear to day 14 post challenge.

To evaluate VIP expression in nonhuman primates (NHP) we transduced *Aotus* monkeys with protective 2A10 VIP construct via efficient rAAV2/1 (rep/cap) vector (data unpublished) and observed the VIP expression kinetics through ELISA.

Vector Plasmid Construct and Cloning

As described, the monoclonal CIS43 [68] and MGU12 [69] antibodies bind upstream of the NANP tetramer repeat region, a region termed the junctional region. CIS43 binds to an epitope 15-mer N'-NPDPNANPNVDPNAN-C' (Peptide 21) and MGU12 binds to 15-mer N'-KQPADGNPDPNANPN-C' (NPDP15) upstream of the central repeat region that gives a different dimension of neutralization uncharted so far.

The first VIP system for the CSP region of the sporozoite used the VIP backbone [62] and the 2A10 and 2C11 [74] variable heavy (V_H) and variable light/kappa (V_K) variable region sequences were cloned as described [62, 65]. To clone the variable regions (referred to as inserts) of the two new antibodies into the 2A10 VIP vector, DNA encoding the published Heavy (V_H) and Light or Kappa (V_K) inserts were first synthesized by Thermo Fisher Invitrogen GeneArt Gene Synthesis. In VIP vectors, the variable regions of the heavy and kappa inserts are flanked by endonuclease restriction

sites, *NotI* and *AgeI* flank the V_H region and *NsiI* and *PstI* flank the V_K region. By different endonuclease reaction and ligation methods, the 2A10 variable insert regions were replaced with the new inserts, as to maintain the functional domains previously described [62, 65].

Using the endonuclease and ligase reactions, the CIS43 V_H and V_K regions were cloned into the VIP plasmids, replacing the 2A10 V_H and V_K regions. CIS43 V_H region was first cloned successfully and confirmed through an additional *DraIII* restriction site that was present in the CIS43 V_H region but not 2A10 V_H region (Fig. 5A). *DraIII* digestion cleaved the CIS43V_H-2A10 V_k plasmid into two fragments, 4444bp and 1986bp in size. However, the cloning procedure for CIS43 V_K did not yield the desired plasmid, therefore Gibson Assembly Kit (New England BioLabs) was used to for V_K cloning. The cloning of CIS43 V_K region into the VIP backbone presented an extra endonuclease *KpnI* restriction site that would give rise to 2 plasmid fragments 5198bp and 1141bp. For the confirmation of the complete integration of both CIS43 V_H and V_K regions, randomly chosen colony lysates after the Gibson Assembly were tested with both *DraIII* and *KpnI* endonuclease to confirm the number of fragment and sizes (Fig.5B). To test for any rare occurrences of mutation during the Gibson Assembly procedure, the restriction enzyme-confirmed CIS43 VIP plasmid was sent to the Johns Hopkins Sequencing Core and confirmed expected integration of CIS43 V_H and V_K inserts and ligation sites.

MGU-12 V_H and V_K regions were cloned into the 2A10-VIP plasmid at the same time by G. Ketner using the Gibson Assembly Kit. Because the restriction sites in variable regions of MGU-12 V_H and V_K would give rise to equal number of fragments and sizes that were too similar to the 2A10-VIP plasmid, the V_H and V_K insert and

ligation sites were sequenced by the Johns Hopkins Sequencing Core and confirmed expected integration of MGU-12 V_H and V_K inserts and ligation sites.

Comparative Functionality of Newly synthesized VIP Plasmid to 2A10 VIP Plasmid in *vitro*

To compare the functionality of the new VIP plasmids, we conducted expression assays on 293T cells in parallel with 2A10 VIP plasmids. Because the 2A10 VIP plasmids have been validated in vitro and vivo, 2A10 VIP plasmid was used as a standard for testing the expression of VIP in 293T cell-line. From the expression assay, CIS43 VIP plasmid had comparable amounts of hIgG secretion while MGU-12 had more than 2-fold production of hIgG (Fig.6). The expression rate of two additional antibody-VIP plasmid was also tested. The CIS43-EIVL VIP plasmid is a construct of CIS43 antibody with amino acids EIVL substituted for the native amino acids DIQM at the amino terminus of the V_k region in an attempt to increase antibody expression (GK, personal communication). Anc-2A10 is an *Aotus nancymae* antibody with C_H and C_K regions of 2A10 replaced with the corresponding regions of *A. nancymaae* IgG (G. Ketner, personal communication). It was hypothesized that IgG with the natural *Aotus* antibody constant regions might be more stable in vivo, and that the expressed antibodies may accumulate to higher concentration in the *Aotus.* However, the CIS43-EIVL and *Aotus*-2A10 additional VIP plasmid constructs had very low expression in comparison to 2A10 VIP (0.018 and 0.035 respectively) and have not been pursued further.

Evaluation of VIP expression kinetics in Murine Model

To evaluate the VIP expression kinetics in vivo, C57/BL6 mice were transduced with rAAV2/8-CIS43 (n=8) and rAAV2/8-MGU-12 (n=9), with rAAV2/8-2A10 as anti-CSP positive control (n=10) and rAAV2/8-b12 (n=10) as anti-CSP negative control (n=10) as 2A10 and b12 VIP was tested previously [62, 65]. Viruses were quantified using qPCR and diluted with TFB2 to achieve $1x10^{11}$ genome copies (GC) in 100uL. 4-6 week old female C57BL6 mice were injected in the right gastrocnemius muscle via insulin syringes. Blood was drawn every week from Week 0 to Week 8 through cheek-bleeds and sera were separated and stored at -80°C. The VIP expression, the anti-CSP antibody was detected by capture with recombinant CSP (rCSP) and HRP-conjugated anti human kappa light chain. Sera were diluted from 1:1,500 in a 3-fold manner to capture the highest dilution that gives twice the amount of background signal in 450nm wavelength (Fig.7).

The highest average anti-CSP antibody expression was from rAAV2/8-MGU-12 (1:1,235,093) (Table 1A), while rAAV2/8-CIS43 showed the lowest average expression of anti-CSP antibody (1:210,230) (Table 1A). From the results, some mice transduced with CIS43 VIP, were considered negative until week 5 and had a rising titer (Fig 7b), however, in these mice, there was detectable signal above the background, however it was short of the threshold for being 'positive' at the lowest dilution of 1:1500. It can be suggested that dilutions lower than 1:1,500 could properly evaluate the concentration of anti-CSP antibody in these mice. The control b12 VIP mice did not produce any detectable concentration of anti-CSP antibody throughout the experimental period.

Transgenic *P.b/P.f*CSP Challenge in Mouse

To evaluate the VIP of its protective efficacy against CSP of *Plasmodium falciparum* in mice, all mice were challenged with the transgenic mouse malaria - *Plasmodium berghei* with the *Plasmodium falciparum* CSP on its surface. For the challenge, A.*stephensii* mosquitoes were blood-fed on blood-stage *Pb/Pf*CSP parasites 21-24 days before the challenge. A day before the challenge, salivary glands of randomly chosen female mosquitoes from the parasite fed mosquito cages were dissected and evaluated for the presence of sporozoites in the salivary gland. In both challenges, the salivary gland infectivity rate of the mosquitoes was over 80% to ensure injection of sporozoites into each mice. 8 weeks post-transduction of rAAV-VIP, each mice was anesthetized with ~100uL of ketamine and were exposed to overnight-starved and dehydrated female *Anopheles stephensii* mosquitoes.

7-11 mosquitoes were placed in individually netted cups and mice were laid on the netted cups until there was visual confirmation of mosquitoes fed over 50%. Post mosquito feeds, all mosquito midgut was dissected to record the number of mosquitoes that fed on each mouse. Between 4-11 mosquitoes fed on each mouse.

Evaluation of VIP expression kinetics in Murine Model #2

After analysis of the first transduction experiment, a replicate experiment was conducted with the same rAAV-VIP vectors. However, due to relatively low levels of anti-CSP hIgG reciprocal dilutions (2A10 – 1:210,230, CIS43 – 46,462, and MGU-12 – 1,235,093)(Table 1A) and protection (10% in only the MGU-12 group)(Fig. 7C) from the

first transduction, $3x10^{11}$ GC were transduced in mice. Because there was a stable expression of antibody after week 2-3, half of the VIP group were bled on either week 1,3 and 8 or week 2, 4 and 8 to capture expression before and after stabilization as well as expression right before the challenge. For the second transduction, the highest average reciprocal titer of anti-CSP antibody was again, rAAV2/8-MGU-12 (1:3,280,500), while rAAV2/8-CIS43 consistently showed the lowest concentration of anti-CSP antibody (1: 465,291) (Table 1B).

The anti-CSP reciprocal titer for all mice transduced with MGU-12 reached the highest dilution in the ELISA assay (1: 3,280,500), and it can be suggested that the mice had higher titers than tested in our ELISA. The negative-control mice transduced with b12 VIP did not produce any detectable concentration of anti-CSP antibody throughout the experimental period.

These mice were also challenged with the transgenic mouse malaria -*Plasmodium berghei* with the *Plasmodium falciparum* CSP on its surface (*Pb/Pf*CSP*)*. The challenge protocol was identical to the first transduction and between 4-11 mosquitoes fed on each mice.

Protection from transgenic *P.b/P.f*CSP Challenge in Mouse

Due to differences in rAAV-VIP GC, the Kaplan-Meier curve was analyzed separately for the replicate challenges. For the first *Pb/Pf*CSP challenge only MGU-12 VIP group showed 10% protection from parasitemia. In the second *Pb/Pf*CSP challenge, CIS43-VIP group showed 10% protection and MGU-12-VIP group showed 50% protection from parasitemia. Both challenges had 100% observed parasitemia from blood smears of the b12-VIP infection-positive control group as well as 2A10-VIP group.

Anti-CSP monoclonal antibodies titer in Non-human Primates transduced with AAV1

The *Aotus* monkey species are a unique family of monkeys that can be naturally infected with human malaria, *P. falciparum* in its sporozoite form [70]. Vaccine models have been studied in *Aotus* monkeys[72] and are able to sustain the parasite lifecycle from sporozoite invasion to transmission through mosquitoes[70]. Because the model can replicate *P.falciparum* sporozoite invasion into the hepatocytes as in humans, it is an ideal model to observe effects of monoclonal antibodies against *P.falciparum* sporozoites.

The 6 monkeys, 3 male and 3 female, were transduced with AAV2/1-2A10 VIP and observed the antibody kinetics up to week 30. AAV1 showed optimal expression efficiency (unpublished data) and was used as the vector for transduction of 2A10-VIP.

On the day of infection, the titrated virus was diluted with 0.1M Citrate 10mM Tris, pH 8.0 (TFB2) solution for the final volume of 200uL. A total of $1x10^{13}$ GC was injected into 6 different sites on the quadricep muscles bilaterally, 3 sites per side.

Post transduction, the monkeys were bled in weeks 1, 2, 3, 4, 6, 8, 11, 15, 20, 25, 30. Identical ELISA protocol for mice was used for the *Aotus* detection of anti-CSP antibody. 2 monkeys and 1 male and 1 female in different pair/cages showed prolonged synthesis of anti-CSP antibody while 4 monkeys showed declines in the level of anti-CSP antibody.

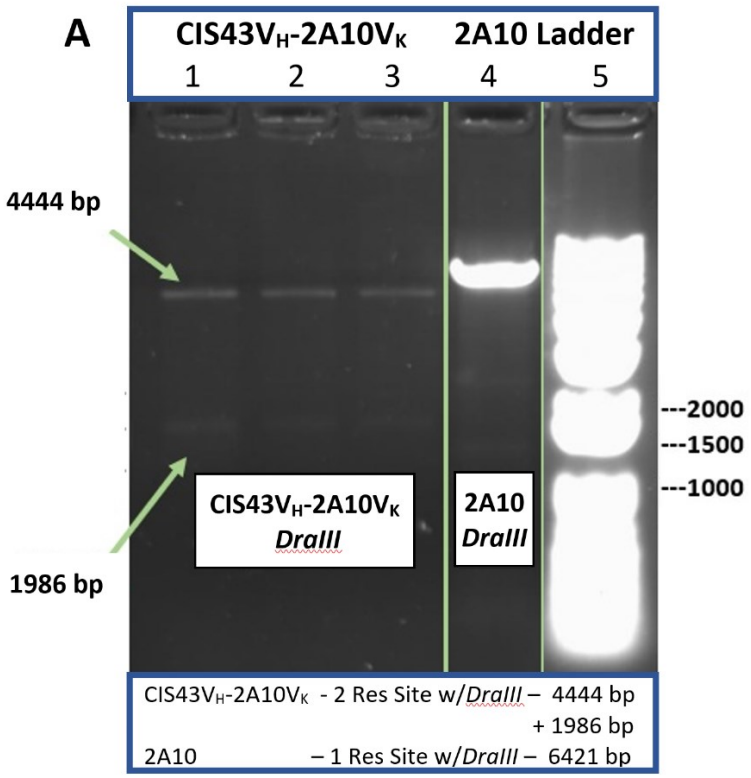
A
CIS43VH-2A10VK
2A10 Ladder
1
2
3
4
5
4444 bp
1986 bp
CIS43VH-2A10VK
DraIII
2A10
DraIII
---2000
---1500
---1000
CIS43VH-2A10VK - 2 Res Site w/DraIII – 4444 bp
+ 1986 bp
2A10 – 1 Res Site w/DraIII – 6421 bp

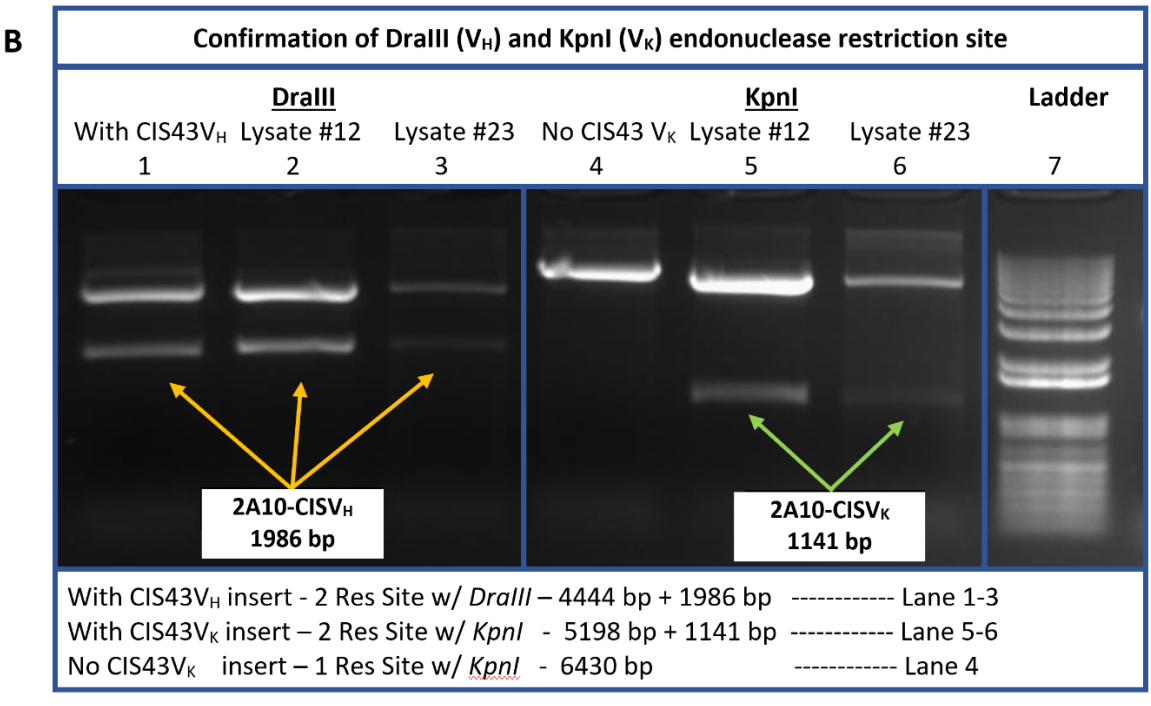
B
Confirmation of DraIII (VH) and KpnI (VK) endonuclease restriction site
DraIII
KpnI
Ladder
With CIS43VH
Lysate #12
Lysate #23
No CIS43 VK
Lysate #12
Lysate #23
1
2
3
4
5
6
7
2A10-CISVH
1986 bp
2A10-CISVK
1141 bp
With CIS43VH insert - 2 Res Site w/ DraIII – 4444 bp + 1986 bp ---------- Lane 1-3
With CIS43VK insert – 2 Res Site w/ KpnI - 5198 bp + 1141 bp ---------- Lane 5-6
No CIS43VK insert – 1 Res Site w/ KpnI - 6430 bp ---------- Lane 4

Figure 5. Confirmation of CIS43V_H-2A10V_K VIP, and CIS43V_H-V_K VIP plasmid by endonuclease reactions

(A) The additional *DraIII* restriction site in the CIS43 V_H region cleaved the plasmid into two fragments, 4444bp and 1986bp in size compared to a linearized 2A10 VIP. Lane 1-3 contains plasmid with CIS43 V_H and 2A10 V_K which results in two fragments. Lane 4 represents plasmid with 2A10 V_H and V_K that only have 1 restriction site resulting in a linearized plasmid. (B) Confirmation of both CIS43 V_H and V_K inserts. Lysate 12 and 23 were digested with either *Dra III* or *KpnI*. Lysates with CIS43 V_H have 2 restriction sites that lead to 2 fragments 4444bp and 1986bp (Lane 2-3). Lysate 12 and 23 were against digested with *KpnI,* which results in 2 fragments in the presence of CIS43V_K. Lysate 12 and 23 show 2 fragments sizes 5198bp and 1141bp that confirms the presence of CIS43 V_K (Lane 5-6). CIS43 V_H-2A10V_K VIP plasmid was used as a positive control for *DraIII* (Lane 1) and negative control for *KpnI* digestion (Lane 4).

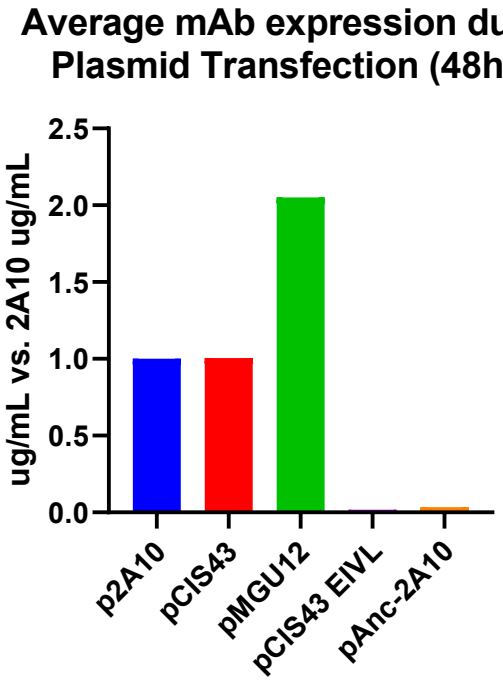

Figure 6. In vitro comparative functionality of the VIP plasmids

The expression efficiencies of CIS43, MGU-12, CIS43-EIVL VIP and *Aotus*-antibody based 2A10 plasmid was evaluated by comparison of human IgG production to the 2A10 VIP. The plasmid concentrations were measured by nanodrop and equal amounts of plasmids were transfected in 293T cell culture with BioT (Bioland Scientific LLC). The supernatant was collected 48 hours post transfection and ELISA was conducted to detect levels of monoclonal hIgG. The expression ratio between 2A10 and other antibodies are CIS43 1:1.006, MGU-12 1:2.051, CIS43-EIVL 1:0.018, Anc-2A10 1:0.035)

A)

VIP Group	Geometric Mean of Reciprocal Dilution
2A10	210,230
CIS43	46,462
MGU-12	1,235,093
b12	0

B)

VIP Group	Geometric Mean of Reciprocal Dilution
2A10	465,291
CIS43	121,433
MGU-12	3,280,500
b12	0

Table 1. Anti-CSP antibody titers

(a) Geometric mean of the reciprocal dilution of the 1st transduction for each VIP group. 2A10 (n=10), CIS43 (n=8), MGU-12 (n=9), b12 (n=10). (b) Geometric mean of the reciprocal dilution of the 2nd transduction for each VIP group. 2A10 (n=10), CIS43 (n=8), MGU-12 (n=9), b12 (n=10).

A

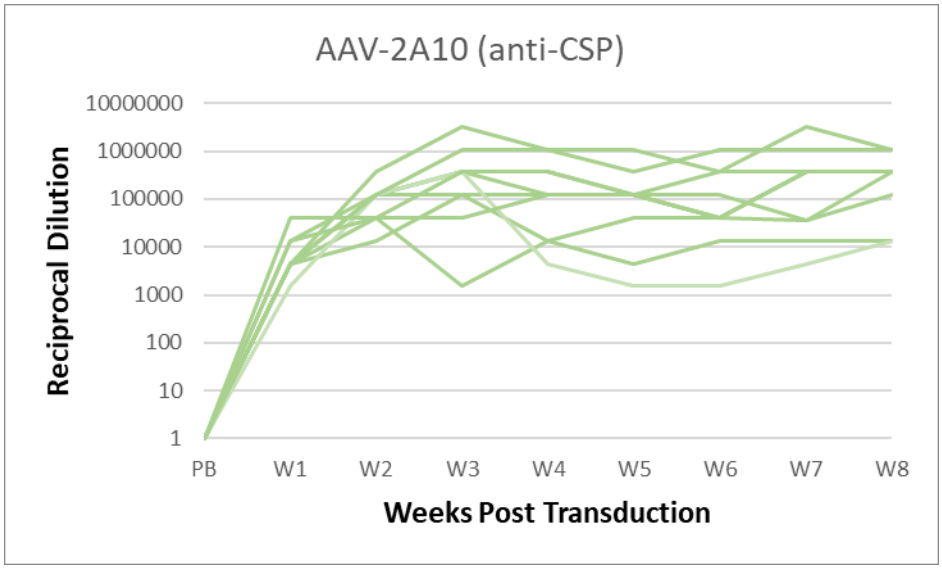
AAV-2A10 (anti-CSP)
Reciprocal Dilution
10000000
1000000
100000
10000
1000
100
10
1
PB
W1
W2
W3
W4
W5
W6
W7
W8
Weeks Post Transduction

B

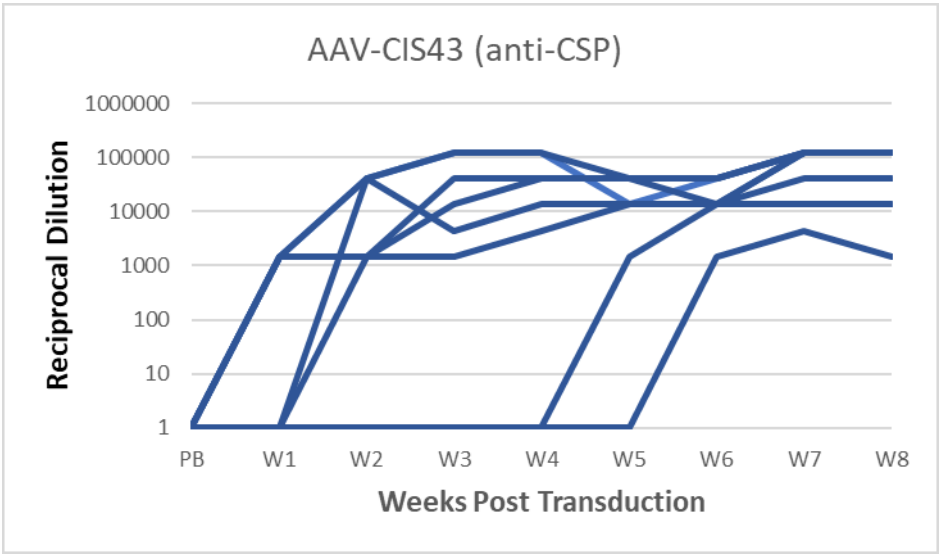
AAV-CIS43 (anti-CSP)
Reciprocal Dilution
1000000
100000
10000
1000
100
10
1
PB
W1
W2
W3
W4
W5
W6
W7
W8
Weeks Post Transduction

C

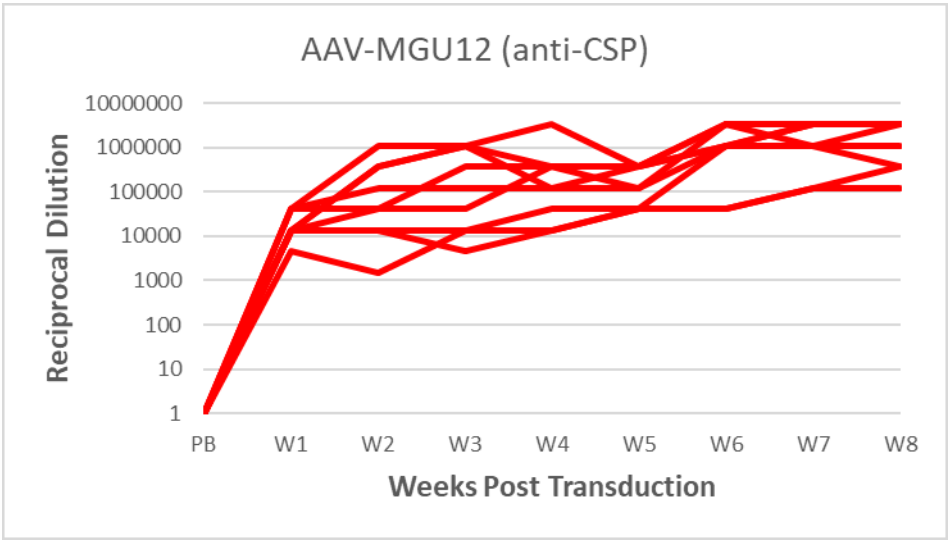
AAV-MGU12 (anti-CSP)
Reciprocal Dilution
10000000
1000000
100000
10000
1000
100
10
1
PB
W1
W2
W3
W4
W5
W6
W7
W8
Weeks Post Transduction

Figure 7. First Transduction: Anti-CSP titers in Mice Transduced by rAAV-VIP

(a) Reciprocal dilution of anti-CSP titer of rAAV-2A10 in individual transduced mice weekly over an 8-week period in log scale (n=8). (a) Reciprocal dilution of anti-CSP titer of rAAV-CIS43 transduced mice over an 8-week period in log scale (n=9). (c) Reciprocal dilution of anti-CSP titer of rAAV-MGU-12 transduced mice over an 8-week period in log scale (n=10). The anti-CSP titer of rAAV-b12 transduced mice did not show any detectable signal and are not shown (n=10).

A

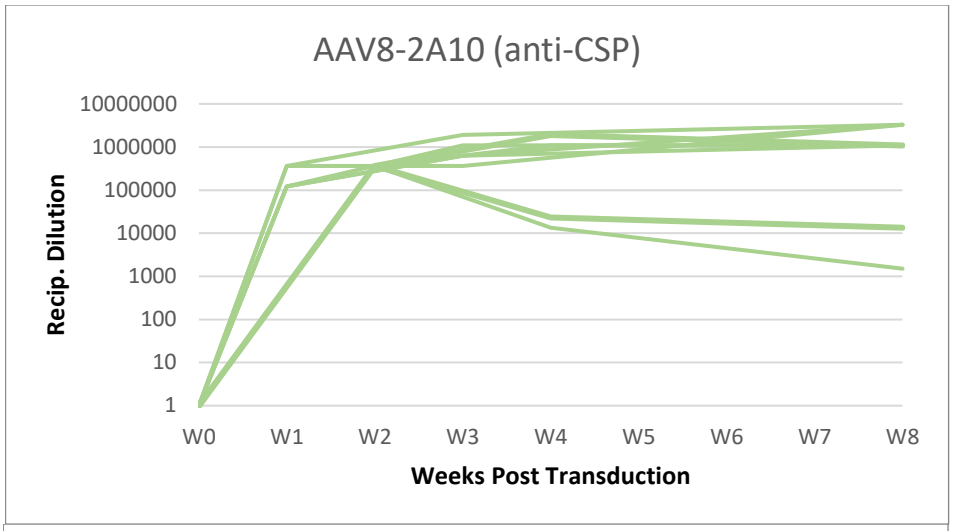
AAV8-2A10 (anti-CSP)
Recip. Dilution
10000000
1000000
100000
10000
1000
100
10
1
W0
W1
W2
W3
W4
W5
W6
W7
W8
Weeks Post Transduction

B

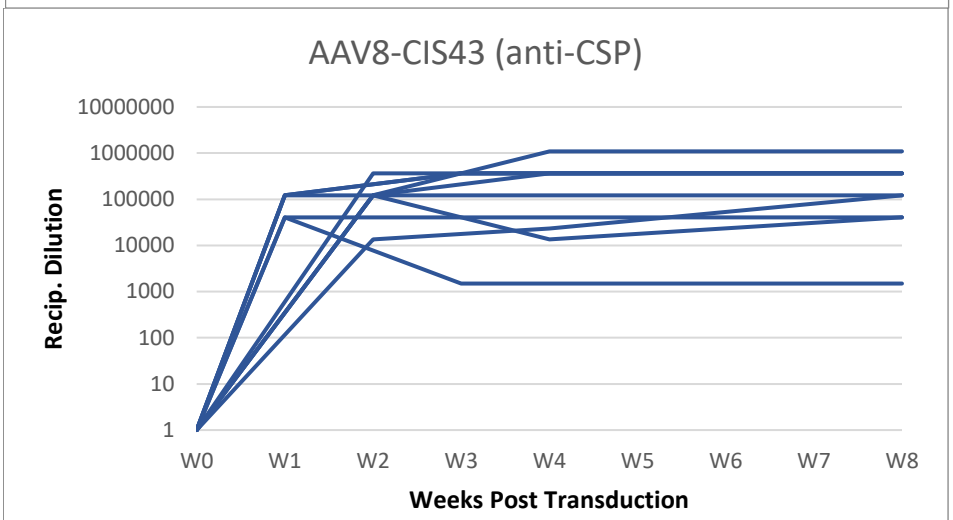
AAV8-CIS43 (anti-CSP)
Recip. Dilution
10000000
1000000
100000
10000
1000
100
10
1
W0
W1
W2
W3
W4
W5
W6
W7
W8
Weeks Post Transduction

C

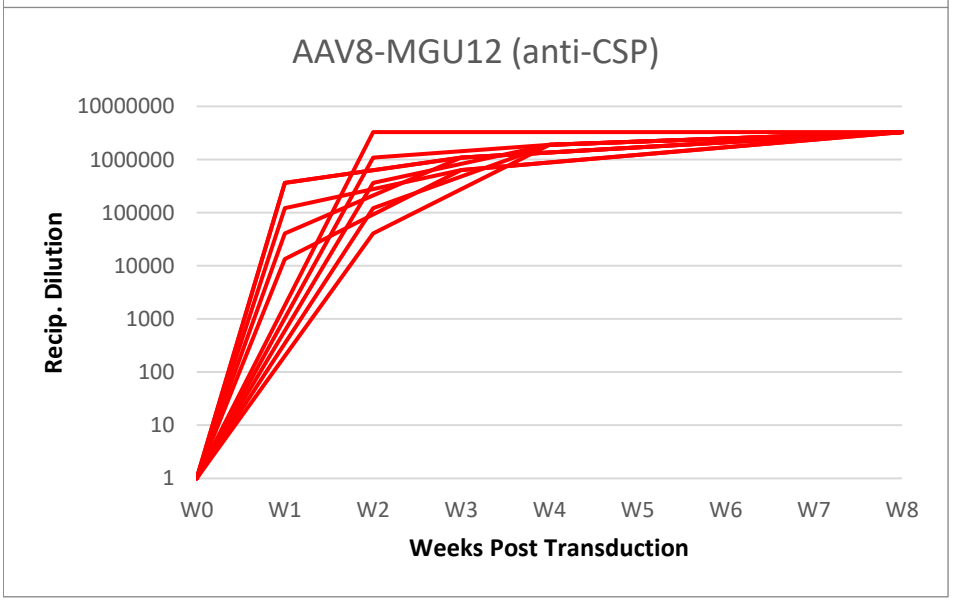
AAV8-MGU12 (anti-CSP)
Recip. Dilution
10000000
1000000
100000
10000
1000
100
10
1
W0
W1
W2
W3
W4
W5
W6
W7
W8
Weeks Post Transduction

Figure 8. Second Transduction: Anti-CSP titer in Mice Transduced by rAAV-VIP

(a) Reciprocal dilution of anti-CSP antibody titer of rAAV-2A10 transduced mice at weeks 1 or 2, 3 or 4 and 8 in a log scale (n=10). (a) Reciprocal dilution of anti-CSP antibody titer of rAAV-CIS43 transduced mice at weeks 1 or 2, 3 or 4 and 8 in log scale (n=9). (c) Reciprocal dilution of anti-CSP antibody titer of rAAV-MGU-12 transduced mice at weeks 1 or 2, 3 or 4 and 8 in a log scale (n=10). The anti-CSP antibody titer of rAAV-b12 transduced mice did not show any detectable signal and are not shown (n=10).

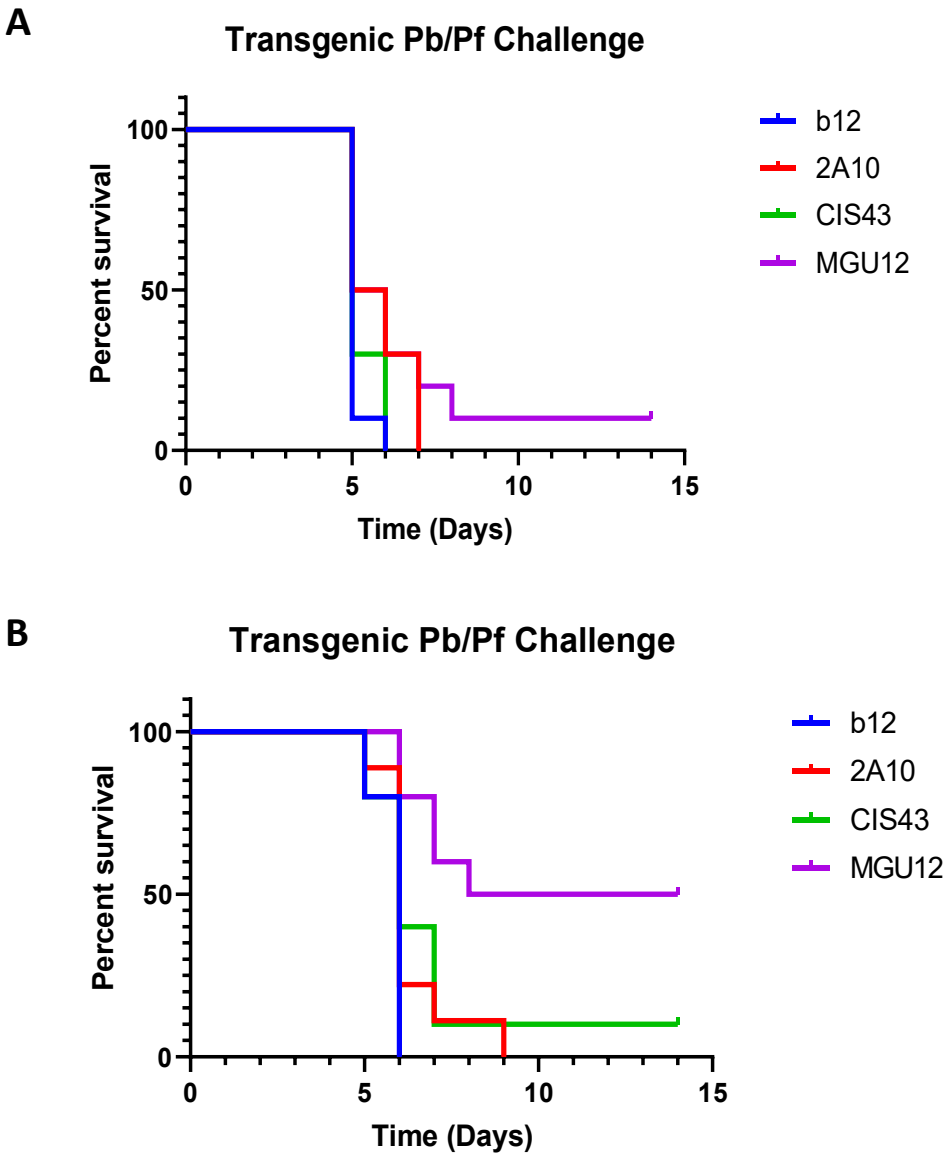

Figure 9. Kaplan-Meier Curve: Days to Patency

(a) During the first *Pb/Pf*CSP challenge, protection from patency was observed in 10% of the MGU-12-VIP mice and while all other mice showed parasitemia by day 8. (b) In the second *Pb/Pf*CSP challenge, protection from patency was observed in 10% of CIS43-VIP group, and 50% of MGU-12 group. In both replicates, the infection-positive control b12-VIP group and 2A10-VIP group had 0% protection from parasitemia observed by blood-smears.

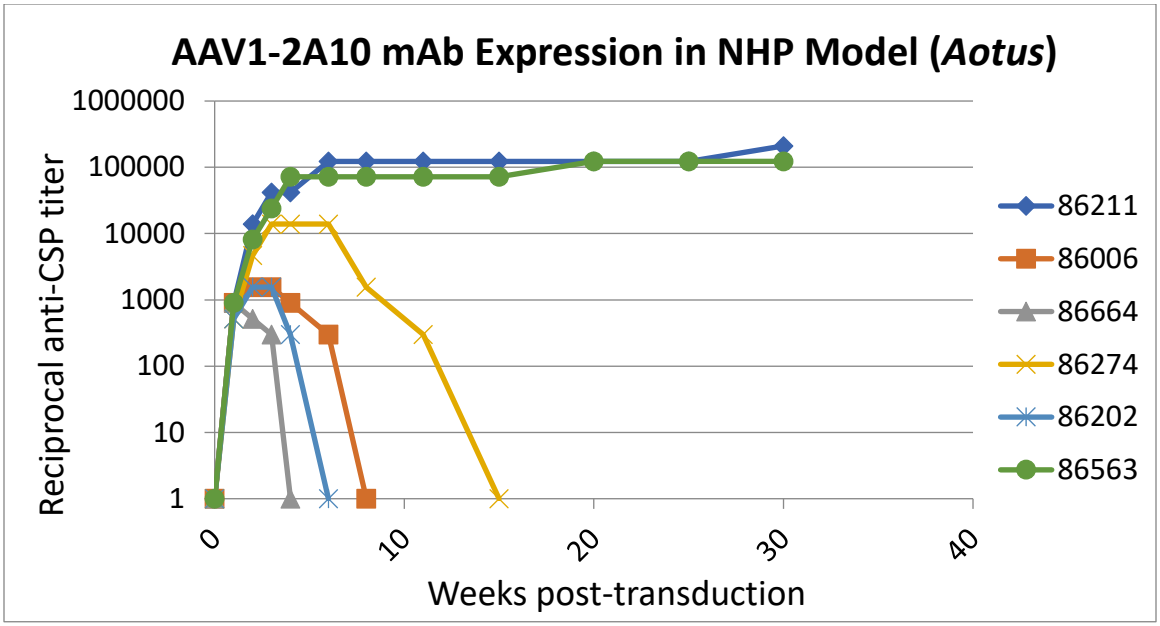

Figure 10. Monoclonal anti-CSP expression in *Aotus* monkeys

The *Aotus* monkeys were transduced using the 2A10/AAV1 vector and blood was drawn from week 0 to week 30 to observe the 2A10-VIP expression. *Aotus* #86211 and #86563 maintained reciprocal dilution of anti-CSP antibody up to 1:210,000 after week 15.

***Aotus* ID**	**Sex**	**Pairs**
86211	F	A
86006	M	
86664	F	B
86274	M	
86202	F	C
86563	M	

Table 2. *Aotus* Sex and Pair Information

Anti-CSP Antibody Reciprocal Dilution											
***Aotus* ID**	**Week 1**	**Week 2**	**Week 3**	**Week 4**	**Week 6**	**Week 8**	**Week 11**	**Week 15**	**Week 20**	**Week 25**	**Week 30**
86211	9.0×10^2	1.4×10^4	4.2×10^4	4.2×10^4	1.2×10^5	1.2×10^5	1.2×10^5	1.2×10^5	1.2×10^5	1.2×10^5	2.1×10^5
86006	9.0×10^2	1.6×10^3	1.6×10^3	9.0×10^2	3.0×10^2	0	0	0	0	0	0
86664	9.0×10^2	5.2×10^2	3.0×10^2	0	0	0	0	0	0	0	0
86274	5.2×10^2	4.7×10^3	1.4×10^4	1.4×10^4	1.4×10^4	1.6×10^3	3.0×10^2	0	0	0	0
86202	5.2×10^2	1.6×10^3	1.6×10^3	3.0×10^2	0	0	0	0	0	0	0
86563	9.0×10^2	8.1×10^3	2.4×10^4	7.2×10^4	7.2×10^4	7.2×10^4	7.2×10^4	7.2×10^4	1.2×10^5	1.2×10^5	1.2×10^5

Table 3. Anti-CSP hIgG Reciprocal Dilution by Week

Discussion

Plasmodium falciparum is a devastating disease that causes over 240 million cases a year especially in developing countries and the major contributor of 266,000 children deaths under 5 years old reported in 2017 [1]. To control the disease, 276 million rapid diagnostic tests, 2.74 billion treatment courses Artemisinin-based combination therapy, and overall, $3.1 billion in resources was used in just 2017 alone to make par with the increasing prominence of the disease [1]. Though decades of research on malaria research has yielded a licensed RTS,S/AS01 malaria vaccine in 2015, the WHO has only recommended the vaccine to a narrow group that have moderate to high malaria endemicity. Moreover, the RTS,S/AS01 vaccine efficacy only provides a moderate vaccine efficacy (35.9%) in its first year, and wanes off completely by year 5 [36]. Though RTS,S/AS01 is a moderately effective vaccine, there is a need for a vaccine with improved efficacy as well as extended period of protection to lessen the burden of infection and reinfection.

From studying and manipulating the immune response against irradiated sporozoites in different animal models and humans [13, 41, 42], as well as data from the phase 3 clinical trial of RTS,S/AS01, the correlate of protection from sporozoite infection was the neutralizing antibody against the CSP antigen [36]. From the data available, increased amount of neutralizing antibody for an extended period would serve as an ideal vaccine against malaria. We have investigated further on expressing high levels of monoclonal antibodies for an extended period by using the VIP system through the AAV vector. In mice, the expression of the antibodies directed against the CSP showed allowed

high titer of antibodies (~1mg/mL) and maintained the level of antibody titer over a year, until the end of the study [65].

VIP system is an AAV vector mediated gene transfer that allows for extended expression and secretion of neutralizing antibodies into the circulation. In our new investigation of VIP system, two 'improved' CSP binding antibodies with higher affinity targeting a region previously unrecognized [68, 69] was integrated into the AAV-VIP system and was evaluated on factors based on mAb expression as well as measure of sterile immunity. The second part of the project involved investigation into the viability of the AAV-VIP system in a nonhuman primate model that could be used directly to test the AAV-VIP against *P. falciparum*, the human malaria parasite.

In characterizing and measuring the expression of the CIS43 [68] and MGU-12 [69] VIP construct, there was a significant difference in expression levels between different antibodies, notably the MGU-12 VIP plasmid expressing more than twice (1:2.051) the amount of antibodies than the 2A10-VIP plasmid (Fig. 6) that was already documented to express high titers of anti-CSP antibodies [65]. This observation was fascinating in two levels, 1) with all components of the VIP system left unedited except for the variable segments there was several fold difference in antibody expression in vitro, and 2) the tested antibody expression in vivo using the rAAV vector had similar correlation as MGU-12-VIP yielded in several fold difference compared to 2A10-VIP (210,230:1,235,095 or ~6:1 ratio in the first mouse transduction and 465,291:3,280,500 or ~7:1 ratio in the second mouse transduction) (Table 1).

Variable expression level is observed in other antibodies as seen in vitro VIP expression data gathered collectively below (Table 2). There is much varied expression

of the transgenes between different VIP constructs as well as the animal model. It is also evident that expression fluctuates with few amino acid changes in the non-variable region as seen from CIS43 VIP, compared to the CIS43 EIVL VIP (Fig. 6). Though the factors for mAb expression rate is uncertain, it has been suggested that the variable region sequences of the VIP construct can contribute to the expression level of the transgene[67].

Publication	Antibody	AAV GC used for Transduction	Antibody quantity ug/mL
Balazs 2012 [62]	B12	$1x10^{11}$	~100
	B12	$1x10^{11}$	20-250
	2G12		
	4E10		
	2F5		
	B12	$1x10^{11}$	10
	B12	$3x10^{9}$-$1x10^{11}$	~0.01-150
	VRC01		~0.1-120
Balazs 2013 [63]	B12	$1x10^{11}$	~100-200
	F10 (anti-H)		~100-200
	CR6261 (anti-H)		0.1-100
	F10 (anti-H)	$5x10^{12}$ /kg	~100
	F10 (anti-H)		>10
	F10 (anti-H)		100X lower than in mice
Deal 2014 [65]	2A10	$1x10^{11}$	~50-1000
	2C11		
	B12		
	2A10		~300-1300
	2C11		~250-750
Balazs 2014 [64]	VRC01	$1x10^{11}$	>100 in sera, 100ng/mL in lamina propria
	VRC07		>100 in sera, 1ug/mL in lamina propria

Table 4. Variable Expression in different VIP constructs

In mice, antibody expression kinetics of rAAV showed stable expression of VIP antibodies, though expression titer was varied among different antibody types (Fig. 7 and 8). The antibody expression peaked between weeks 2-4 and was maintained at similar titers until week 8 before the *Pb/Pf*CSP challenge.

In measuring patency and protection following the *Pb/Pf*CSP challenge, highest survival rate was observed in mice group with the highest reciprocal titer (MGU-12, 1:1,235,093 in first transduction and 1:3,280,500 in second transduction) (Fig.7 and 8). The MGU-12 VIP group achieved the highest reciprocal titer tested by ELISA, and of those that reached the maximum reciprocal titer of $3.28x10^6$ in the second transduction 5/10 were protected (Fig. 8C). From both CIS43-VIP groups from two challenges, the one mouse that survived the *Pb/Pf*CSP challenge had the second highest anti-CSP antibody titer ($1:3.65x10^5$) (Fig. 8B). In both the MGU-12 VIP groups from two challenges, protection from *Pb/Pf*CSP was only observed in mice with titers at $1:3.28x10^6$ anti-CSP antibody titer (Fig. 7C and 8C). Though it is not conclusive due to low sample size, it could be suggested that lower concentration of CIS43-VIP could elicit similar or higher rate of protection than MGU-12 VIP. In the 2A10-VIP group, the antibody titer was much lower than MGU-12, averaging $2.10x10^5$ in the first transduction and $4.65x10^5$ in the second transduction (Table 1) and no protection was observed in contrast to the past findings. [65]. Though the main reasons for this result is uncertain, factors such as different parasite strain and method for intramuscular injections resulting in less efficient infection could elicit low expression and protection, and consistency in the control VIP may be needed to further support the finding. In addition, further

investigations into actual antibody quantity may reveal the efficacy of the antibody as well as efficiency of the rAAV vectors.

In transduction of the *Aotus* monkeys, all 6 monkeys were transduced with AAV1 VIP vectors that encoded the 2A10 antibody heavy and kappa variable regions. Different capsids were tested in *Aotus* models and showed that AAV1 had the highest capacity (unpublished data) to deliver the transgene into the nonhuman primates. In the first 2 weeks post transduction, all 6 monkeys saw rising anti-CSP hIgG titers (Fig. 10). However, from week 3, signs of hIgG decline was evident and by week 6, 3/6 of the *Aotus* (#86211, 86006, 86664) showed no detectable hIgG. At the end of week 30, 2/6 monkeys still maintained an elevated level ($1:2.1x10^5$ in #86211 and $1:1.2x10^5$ in #86563) of anti-CSP hIgG (Fig. 10). Though upon stabilization of the transgene expression, the level of antibody titer was encouraging, however, the percentage of monkeys that had sudden declining titers showed the need for further research in realizing the full potential of the VIP system.

Due to report of pre-existing immunity against ubiquitous AAV[75], efforts in optimizing AAV vectors have been explored, which include directed evolution/mutation of the capsid, discovery of naturally occurring AAV, rational design of AAV from existing strains and in silico design of AAV capsids through computational approaches [45]. Development of 'unseen' AAV vectors would not only circumvent pre-existing immunity, but it could also open doors to developing therapies that require sequential delivery or multi-dose or re-administration of transgenes as a booster dose.

Specific improvements for VIP and antibody transgene delivery have also been investigated due to reports of host immune responses that elicit anti-drug antibodies

(ADA) in NHP [67, 76, 77]. Progress has also been made against ADA, such as the use of pharmacological molecules to such as cyclosporine [67] and rituximab [78] that elicit immunosuppression of subjects and allow undisrupted expression and functionality of the transgene. In addition, continuous investigations on antibody structure/affinity are ongoing, including discovery of higher affinity antibodies through CHIM [68, 69], engineering the structural make-up of antibodies for extended duration of half-life [79, 80], and expressing cocktail of antibodies targeting different part of the CSP.

However, as interest in AAV and gene therapy grows, further considerations for safety, and cost needs to be considered in the scope of public health. Though an AAV-based gene therapy products are available, new information on rAAV-induced side effects are still unraveling [81] and further investigations on gene- insertion related issues [82] have raised an alert for use of AAV in a clinical setting. Therefore, further observation, investigation and careful regulation needs to be instituted for drug safety.

It is also concerning that the cost of the first two approved gene therapy is astronomical. According to news sources in the US and Europe, Glybera costs €1 million ($1.2m) and Luxturna costs $850,000, $425,000 per eye. It is two most expensive drugs in the world, and due to its cost, Glybera, which has been licensed since 2012, has only had 1 patient and is no longer in the market as there is no demand for the drug. For further evaluation of AAV as drugs, propaganda for AAV drug safety and to actually influence public health, the pharmaceutical industry needs to make compromises for continuation of AAV-based drugs.

Our current model of the VIP system against the sporozoite stage of *P.falciparum* has shown evidence of efficient delivery vector and demonstrated potent antibodies in

achieving sterile immunity. However, further investigations into neutralizing antibodies, AAV vectors and challenge models in nonhuman primates are needed to further validate the VIP system and to potentially play a part in alleviation of the burden of malaria and eliminating the disease in the long term.

References

1. WHO. *Malaria*. 2019 [cited 2019 Mar 17]; Available from: https://www.who.int/malaria/en/.
2. WHO, *Artemisinin and artemisinin-based combination therapy resistance.* 2017.
3. Zuber, J.A. and S. Takala-Harrison, *Multidrug-resistant malaria and the impact of mass drug administration.* Infect Drug Resist, 2018. **11**: p. 299-306.
4. Organization, W.H., *World Malaria Report 2017*. 2017: November 2017.
5. Cox, F.E., *History of the discovery of the malaria parasites and their vectors.* Parasites & Vectors, 2010. **3**(1): p. 5.
6. Yamauchi, L.M., et al., *Plasmodium sporozoites trickle out of the injection site.* Cell Microbiol, 2007. **9**(5): p. 1215-22.
7. Flores-Garcia, Y., et al., *Antibody-Mediated Protection against Plasmodium Sporozoites Begins at the Dermal Inoculation Site.* MBio, 2018. **9**(6).
8. Sinnis, P. and F. Zavala, *The skin stage of malaria infection: biology and relevance to the malaria vaccine effort.* Future Microbiol, 2008. **3**(3): p. 275-8.
9. Cowman, A.F., et al., *Malaria: Biology and Disease.* Cell, 2016. **167**(3): p. 610-624.
10. Cowman, A.F., et al., *The Molecular Basis of Erythrocyte Invasion by Malaria Parasites.* Cell Host Microbe, 2017. **22**(2): p. 232-245.
11. Long, C.A. and F. Zavala, *Immune Responses in Malaria.* Cold Spring Harb Perspect Med, 2017. **7**(8).
12. Long, C.A. and F. Zavala, *Malaria vaccines and human immune responses.* Curr Opin Microbiol, 2016. **32**: p. 96-102.
13. Zavala, F., et al., *Rationale for development of a synthetic vaccine against Plasmodium falciparum malaria.* Science, 1985. **228**(4706): p. 1436-40.

14. Medica, D.L. and P. Sinnis, *Quantitative dynamics of Plasmodium yoelii sporozoite transmission by infected anopheline mosquitoes.* Infect Immun, 2005. **73**(7): p. 4363-9.

15. Amino, R., et al., *Quantitative imaging of Plasmodium transmission from mosquito to mammal.* Nat Med, 2006. **12**(2): p. 220-4.

16. Nussenzweig, R.S., et al., *Protective immunity produced by the injection of x-irradiated sporozoites of plasmodium berghei.* Nature, 1967. **216**(5111): p. 160-2.

17. Rieckmann, K.H., et al., *Use of attenuated sporozoites in the immunization of human volunteers against falciparum malaria.* Bull World Health Organ, 1979. **57 Suppl 1**: p. 261-5.

18. Kariu, T., et al., *CelTOS, a novel malarial protein that mediates transmission to mosquito and vertebrate hosts.* Mol Microbiol, 2006. **59**(5): p. 1369-79.

19. Robson, K.J., et al., *A highly conserved amino-acid sequence in thrombospondin, properdin and in proteins from sporozoites and blood stages of a human malaria parasite.* Nature, 1988. **335**(6185): p. 79-82.

20. Rogers, W.O., et al., *Characterization of Plasmodium falciparum sporozoite surface protein 2.* Proc Natl Acad Sci U S A, 1992. **89**(19): p. 9176-80.

21. Douglas, R.G., et al., *Active migration and passive transport of malaria parasites.* Trends Parasitol, 2015. **31**(8): p. 357-62.

22. Ejigiri, I., et al., *Shedding of TRAP by a rhomboid protease from the malaria sporozoite surface is essential for gliding motility and sporozoite infectivity.* PLoS Pathog, 2012. **8**(7): p. e1002725.

23. Guerin-Marchand, C., et al., *A liver-stage-specific antigen of Plasmodium falciparum characterized by gene cloning.* Nature, 1987. **329**(6135): p. 164-7.

24. Tiono, A.B., et al., *First field efficacy trial of the ChAd63 MVA ME-TRAP vectored malaria vaccine candidate in 5-17 months old infants and children.* PLoS One, 2018. **13**(12): p. e0208328.

25. Domarle, O., et al., *Factors influencing resistance to reinfection with Plasmodium falciparum.* Am J Trop Med Hyg, 1999. **61**(6): p. 926-31.

26. John, C.C., et al., *Correlation of high levels of antibodies to multiple pre-erythrocytic Plasmodium falciparum antigens and protection from infection.* Am J Trop Med Hyg, 2005. **73**(1): p. 222-8.

27. Nussenzweig, V. and R.S. Nussenzweig, *Rationale for the development of an engineered sporozoite malaria vaccine.* Adv Immunol, 1989. **45**: p. 283-334.

28. Zavala, F., et al., *Circumsporozoite proteins of malaria parasites contain a single immunodominant region with two or more identical epitopes.* J Exp Med, 1983. **157**(6): p. 1947-57.

29. Zavala, F., et al., *Ubiquity of the repetitive epitope of the CS protein in different isolates of human malaria parasites.* J Immunol, 1985. **135**(4): p. 2790-3.

30. Plassmeyer, M.L., et al., *Structure of the Plasmodium falciparum circumsporozoite protein, a leading malaria vaccine candidate.* J Biol Chem, 2009. **284**(39): p. 26951-63.

31. Coppi, A., et al., *The Plasmodium circumsporozoite protein is proteolytically processed during cell invasion.* J Exp Med, 2005. **201**(1): p. 27-33.

32. Coppi, A., et al., *The malaria circumsporozoite protein has two functional domains, each with distinct roles as sporozoites journey from mosquito to mammalian host.* J Exp Med, 2011. **208**(2): p. 341-56.

33. Seder, R.A., et al., *Protection against malaria by intravenous immunization with a nonreplicating sporozoite vaccine.* Science, 2013. **341**(6152): p. 1359-65.

34. Cohen, J., et al., *From the circumsporozoite protein to the RTS, S/AS candidate vaccine.* Hum Vaccin, 2010. **6**(1): p. 90-6.

35. Kester, K.E., et al., *Randomized, double-blind, phase 2a trial of falciparum malaria vaccines RTS,S/AS01B and RTS,S/AS02A in malaria-naive adults: safety, efficacy, and immunologic associates of protection.* J Infect Dis, 2009. **200**(3): p. 337-46.

36. Olotu, A., et al., *Seven-Year Efficacy of RTS,S/AS01 Malaria Vaccine among Young African Children.* N Engl J Med, 2016. **374**(26): p. 2519-29.

37. Neafsey, D.E., et al., *Genetic Diversity and Protective Efficacy of the RTS,S/AS01 Malaria Vaccine.* N Engl J Med, 2015. **373**(21): p. 2025-2037.

38. Collins, K.A., et al., *Enhancing protective immunity to malaria with a highly immunogenic virus-like particle vaccine.* Sci Rep, 2017. **7**: p. 46621.

39. White, M.T., et al., *The relationship between RTS,S vaccine-induced antibodies, CD4(+) T cell responses and protection against Plasmodium falciparum infection.* PLoS One, 2013. **8**(4): p. e61395.

40. White, M.T., et al., *Immunogenicity of the RTS,S/AS01 malaria vaccine and implications for duration of vaccine efficacy: secondary analysis of data from a phase 3 randomised controlled trial.* Lancet Infect Dis, 2015. **15**(12): p. 1450-8.

41. Foquet, L., et al., *Vaccine-induced monoclonal antibodies targeting circumsporozoite protein prevent Plasmodium falciparum infection.* J Clin Invest, 2014. **124**(1): p. 140-4.

42. Hollingdale, M.R., et al., *Age-dependent occurrence of protective anti-Plasmodium falciparum sporozoite antibodies in a holoendemic area of Liberia.* Trans R Soc Trop Med Hyg, 1989. **83**(3): p. 322-4.

43. Espinosa, D.A., et al., *Proteolytic Cleavage of the Plasmodium falciparum Circumsporozoite Protein Is a Target of Protective Antibodies.* J Infect Dis, 2015. **212**(7): p. 1111-9.

44. Sack, B.K., et al., *Model for in vivo assessment of humoral protection against malaria sporozoite challenge by passive transfer of monoclonal antibodies and immune serum.* Infect Immun, 2014. **82**(2): p. 808-17.

45. Wang, D., P.W.L. Tai, and G. Gao, *Adeno-associated virus vector as a platform for gene therapy delivery.* Nat Rev Drug Discov, 2019.

46. Fields, B.N., D.M. Knipe, and P.M. Howley, *Fields virology*. 2013, Philadelphia: Wolters Kluwer Health/Lippincott Williams & Wilkins.

47. Sonntag, F., et al., *The assembly-activating protein promotes capsid assembly of different adeno-associated virus serotypes.* J Virol, 2011. **85**(23): p. 12686-97.

48. Pillay, S., et al., *An essential receptor for adeno-associated virus infection.* Nature, 2016. **530**(7588): p. 108-12.

49. Pillay, S., et al., *Adeno-associated Virus (AAV) Serotypes Have Distinctive Interactions with Domains of the Cellular AAV Receptor.* J Virol, 2017. **91**(18).

50. Summerford, C., J.S. Johnson, and R.J. Samulski, *AAVR: A Multi-Serotype Receptor for AAV.* Mol Ther, 2016. **24**(4): p. 663-6.

51. Bartlett, J.S., R. Wilcher, and R.J. Samulski, *Infectious entry pathway of adeno-associated virus and adeno-associated virus vectors.* J Virol, 2000. **74**(6): p. 2777-85.

52. Sonntag, F., et al., *Adeno-associated virus type 2 capsids with externalized VP1/VP2 trafficking domains are generated prior to passage through the cytoplasm and are maintained until uncoating occurs in the nucleus.* J Virol, 2006. **80**(22): p. 11040-54.

53. Xiao, P.J. and R.J. Samulski, *Cytoplasmic trafficking, endosomal escape, and perinuclear accumulation of adeno-associated virus type 2 particles are facilitated by microtubule network.* J Virol, 2012. **86**(19): p. 10462-73.

54. Kotin, R.M., et al., *Mapping and direct visualization of a region-specific viral DNA integration site on chromosome 19q13-qter.* Genomics, 1991. **10**(3): p. 831-4.

55. Dong, J.Y., P.D. Fan, and R.A. Frizzell, *Quantitative analysis of the packaging capacity of recombinant adeno-associated virus.* Hum Gene Ther, 1996. **7**(17): p. 2101-12.

56. Duan, D., et al., *Circular intermediates of recombinant adeno-associated virus have defined structural characteristics responsible for long-term episomal persistence in muscle tissue.* J Virol, 1998. **72**(11): p. 8568-77.

57. Fisher, K.J., et al., *Transduction with recombinant adeno-associated virus for gene therapy is limited by leading-strand synthesis.* J Virol, 1996. **70**(1): p. 520-32.

58. Ferrari, F.K., et al., *Second-strand synthesis is a rate-limiting step for efficient transduction by recombinant adeno-associated virus vectors.* J Virol, 1996. **70**(5): p. 3227-34.

59. McCarty, D.M., et al., *Adeno-associated virus terminal repeat (TR) mutant generates self-complementary vectors to overcome the rate-limiting step to transduction in vivo.* Gene Ther, 2003. **10**(26): p. 2112-8.

60. Yla-Herttuala, S., *Endgame: glybera finally recommended for approval as the first gene therapy drug in the European union.* Mol Ther, 2012. **20**(10): p. 1831-2.

61. FDA. *FDA Approves novel gene therapy to treat patients with a rare form of inherited vision loss*. 2017 [cited 2019 April 20, 2019]; Available from: https://www.fda.gov/newsevents/newsroom/pressannouncements/ucm589467.htm.

62. Balazs, A.B., et al., *Antibody-based protection against HIV infection by vectored immunoprophylaxis.* Nature, 2011. **481**(7379): p. 81-4.

63. Balazs, A.B., et al., *Broad protection against influenza infection by vectored immunoprophylaxis in mice.* Nat Biotechnol, 2013. **31**(7): p. 647-52.

64. Balazs, A.B., et al., *Vectored immunoprophylaxis protects humanized mice from mucosal HIV transmission.* Nat Med, 2014. **20**(3): p. 296-300.

65. Deal, C., et al., *Vectored antibody gene delivery protects against Plasmodium falciparum sporozoite challenge in mice.* Proc Natl Acad Sci U S A, 2014. **111**(34): p. 12528-32.

66. Deal, C.E. and A.B. Balazs, *Vectored antibody gene delivery for the prevention or treatment of HIV infection.* Curr Opin HIV AIDS, 2015. **10**(3): p. 190-7.

67. Saunders, K.O., et al., *Broadly Neutralizing Human Immunodeficiency Virus Type 1 Antibody Gene Transfer Protects Nonhuman Primates from Mucosal Simian-Human Immunodeficiency Virus Infection.* J Virol, 2015. **89**(16): p. 8334-45.

68. Kisalu, N.K., et al., *A human monoclonal antibody prevents malaria infection by targeting a new site of vulnerability on the parasite.* Nat Med, 2018. **24**(4): p. 408-416.

69. Tan, J., et al., *A public antibody lineage that potently inhibits malaria infection through dual binding to the circumsporozoite protein.* Nat Med, 2018. **24**(4): p. 401-407.

70. Collins, W.E., et al., *The Santa Lucia strain of Plasmodium falciparum in Aotus monkeys.* Am J Trop Med Hyg, 2009. **80**(4): p. 536-40.

71. Hayton, K., et al., *Erythrocyte binding protein PfRH5 polymorphisms determine species-specific pathways of Plasmodium falciparum invasion.* Cell Host Microbe, 2008. **4**(1): p. 40-51.

72. Srinivasan, P., et al., *A malaria vaccine protects Aotus monkeys against virulent Plasmodium falciparum infection.* NPJ Vaccines, 2017. **2**.

73. Saraiva, J., R.J. Nobre, and L. Pereira de Almeida, *Gene therapy for the CNS using AAVs: The impact of systemic delivery by AAV9.* J Control Release, 2016. **241**: p. 94-109.

74. Zavala, F., et al., *Monoclonal antibodies to circumsporozoite proteins identify the species of malaria parasite in infected mosquitoes.* Nature, 1982. **299**(5885): p. 737-8.

75. Calcedo, R., et al., *Worldwide epidemiology of neutralizing antibodies to adeno-associated viruses.* J Infect Dis, 2009. **199**(3): p. 381-90.

76. Gardner, M.R., et al., *Anti-drug Antibody Responses Impair Prophylaxis Mediated by AAV-Delivered HIV-1 Broadly Neutralizing Antibodies.* Mol Ther, 2019.

77. Martinez-Navio, J.M., et al., *Host Anti-antibody Responses Following Adeno-associated Virus-mediated Delivery of Antibodies Against HIV and SIV in Rhesus Monkeys.* Mol Ther, 2016. **24**(1): p. 76-86.

78. Mingozzi, F., et al., *Pharmacological modulation of humoral immunity in a nonhuman primate model of AAV gene transfer for hemophilia B.* Mol Ther, 2012. **20**(7): p. 1410-6.

79. Dall'Acqua, W.F., P.A. Kiener, and H. Wu, *Properties of human IgG1s engineered for enhanced binding to the neonatal Fc receptor (FcRn).* J Biol Chem, 2006. **281**(33): p. 23514-24.

80. Zalevsky, J., et al., *Enhanced antibody half-life improves in vivo activity.* Nat Biotechnol, 2010. **28**(2): p. 157-9.

81. Hinderer, C., et al., *Severe Toxicity in Nonhuman Primates and Piglets Following High-Dose Intravenous Administration of an Adeno-Associated Virus Vector Expressing Human SMN.* Hum Gene Ther, 2018. **29**(3): p. 285-298.

82. Nault, J.C., et al., *Recurrent AAV2-related insertional mutagenesis in human hepatocellular carcinomas.* Nat Genet, 2015. **47**(10): p. 1187-93.

Curriculum Vitae

Suk Namkung
Snamkun2@jhu.edu
Date of Birth: Dec 10, 1989
Place of Birth: Seoul, South Korea

Johns Hopkins Bloomberg School of Public Health
Department of Molecular Microbiology and Immunology
615 N. Wolfe Street
Baltimore, MD 21205

15 Charles Plaza #1303
Baltimore, MD 21201
T: +1-667-201-9074

Education

2017-2019 **Johns Hopkins Bloomberg School of Public Health**
ScM, Department of Molecular Microbiology and Immunology

Thesis: Adeno-associated virus vectored immunoprophylaxis against human malaria *Plasmodium falciparum*: Murine and Nonhuman primate model

2008-2012 **Baylor University**
BS, Biology, Chemistry and Medical Humanities Minor

Research / Laboratory experience

2017-present **Johns Hopkins Bloomberg School of Public Health,** Baltimore, MD
Graduate student; Advisor: Gary Ketner
Thesis: Adeno-associated Virus vectored immunoprophylaxis against human malaria: Murine and Non-Human Primate Model

2014-2017 **International Vaccine Institute (Global Dengue and Aedes-Transmitted Diseases Consortium, previously Dengue Vaccine Initiative),** Seoul, South Korea
Research Assistant; Program Director: Inkyu Yoon
Measuring the burden of Dengue in Africa: Fever surveillance, Serological survey, Cost-of-illness survey and Healthcare utilization survey

2009-2012 **Baylor University,** Waco, TX
Undergraduate Researcher; Advisor: Patrick Danley
Phylogenetic analysis of Oedipodinae Grasshopper species from the Old World and the New World

2010-2012 **Baylor University,** Waco, TX
Undergraduate Researcher; Advisor: Tamarah Adair
Studied possible correlation between Bacteriophage K infectivity and antibiotic resistance

2006-2010 **Bethesda Medical Center,** Kampala, Uganda
Summer intern; Supervisor: Luke Hyunsuk Lim
Shadowed laboratory technician and conducted diagnostic and laboratory tests for parasites and bacteria

Publications

2017 *Lim, J.K., Carabali M., Lee J.S., Lee K.S., **Namkung S**. et al. (2017). Evaluating dengue burden in Africa in passive fever surveillance and seroprevalence studies: protocol of field studies of the Dengue Vaccine Initiative. BMJ Open, 8(1): e017673*

2016 *Lim, S. K., Lee, Y.S., **Namkung, S.**, Lim, J.K., & Yoon, I.K. (2016). Prospects for dengue vaccines for travelers. Clin Exp Vaccine Res, 5(2), 89-100.*

2015 *Husemann, M., Habel, J.C., **Namkung, S.,** Hochkirch, A., Otte, D., & Danley, P.D. (2015) Molecular evidence for an old world origin of Galapagos and Caribbean band-winged grasshoppers (Acrididae: Oedipodinae: Sphingonotus). PloS One, 10(2), e0118208*

2012 Husemann, M., **Namkung, S.,** Habel, J.C., Danley, P.D. & Hochkirch, A. (2012). Phylogenetic analyses of band-winged grasshoppers (Orthoptera, Acrididae, Oedipodinae) reveal convergence of wing morphology. —*Zoologica Scripta*, *41*, 515–526

Presentations and Seminars

2019 **Namkung, S**. and Ketner, G. Adeno-associated virus vectored immunoprophylaxis against human malaria parasite: in Murine and Nonhuman primate model. Poster presentation, World Malaria Day, Baltimore, MD

2012 **Namkung, S**., Husemann, M., and Danley, P. **Evolutionary relationships of Oedipodinae grasshoppers revealed through molecular analysis.** Oral Presentation, Baylor University Graduate Seminar, Waco, TX

2011 **Namkung, S**. and Adair, T. ***Phage K Infectivity of Staphylococcus aureus isolated from healthy carriers.*** Poster presentation, American Society of Microbiology, Texas Branch, New Braunfels, TX

2011 **Namkung, S**., Husemann, M., and Danley, P. ***Common Ancestry or Convergence? Evolution of Wing Morphology in Band-winged Grasshoppers.*** *Poster presentation, Baylor Undergraduate Research and Scholarly Achievement, Waco, TX*

Scholarships / Awards

2010 ***Baylor University Undergraduate Research and Scholarly Achievement (URSA) Grant & Award***
Baylor University, Waco, Texas
2010 - *Investigation of community based, naturally occurring phage-resistant Staphylococcus aureus*
2010 - *Parallel Speciation or Common Ancestry? – Evolution of Diversity in New and Old World*
Genera of Band-Winged Grasshoppers

2008-2012 ***Baylor Provost's Gold Scholarship***
Baylor University, Waco, Texas

Employment

2017-present	**Laboratory Assistant** Johns Hopkins Bloomberg School of Public Health, Baltimore, MD *Department of Molecular Microbiology and Immunology*
2012-2014	**Enlisted Soldier, Republic of Korea Army** Camp Casey, South Korea Served in the Korean Augmentation to the United States Army (KATUSA Program) in 210th Fires Brigade (now Field Artillery Brigade) as a translator during the compulsory Korean military service.
2009-2012	**Laboratory Assistant** Baylor University, Waco, Texas

Professional Training / Certificate

2017-2019 (expected)	**Certificate in Vaccine Science and Policy** Johns Hopkins Bloomberg School of Public Health Department of International Health
2014 & 2017	**CITI Good Clinical Practice (GCP)** International Vaccine Institute
2015	**IVI Vaccinology Course** International Vaccine Institute

References

Gary Ketner Ph.D
Professor, Department of Molecular Microbiology and Immunology
Johns Hopkins Bloomberg School of Public Health
615 N. Wolfe Street
Baltimore, MD 21205
E: gketner1@jhu.edu
T: +1-410-955-3776

In Kyu Yoon MD
Director, Global Dengue & Aedes-Transmitted Diseases Consortium (GDAC)
International Vaccine Institute
Seoul National Univ. Research Park
1 Gwanak-ro, Gwanak-gu, Seoul, South Korea
E: Inkyu.yoon@ivi.int
T: +1-240-422-0935

Prakash Srinivasan Ph.D
Assistant Professor, Department of Molecular Microbiology and Immunology
Johns Hopkins Bloomberg School of Public Health
615 N. Wolfe Street
Baltimore, MD 21205
E: psriniv3@jhu.edu
T: +1-443-287-3097